ABSTRACT

Title of Document: EFFECT OF JOULE HEATING ON THE RELIABILITY OF STAMPED METAL LAND GRID ARRAY SOCKETS

Vidyullatha Challa, PhD, 2010

Directed By: Professor Michael Pecht, Department of Mechanical Engineering

Performance requirements in high end microprocessors have increased tremendously in the last several years, leading to higher I/O counts and interconnect densities. As greater currents pass through the microprocessor interconnect, higher temperatures driven by Joule heating are expected to pose reliability risks to high pin count microprocessor sockets. In this study Joule heating and its effect on the reliability of stamped metal land grid array (LGA) sockets was investigated using a combination of experimental and numerical methods. A methodology to determine socket temperature environments under electrical loading was developed. Knowledge of socket operating temperatures can allow original equipment manufacturers (OEMs) and socket manufacturers to test for and mitigate failure mechanisms under thermal aging.

The factors that influence Joule heating and contribute to premature socket failure were examined. Processor temperature, contact alloy and contact pitch were

all found to significantly influence socket temperatures driven by Joule heating, with the contact alloy and processor temperature having the most significant effects. The resulting temperatures at higher currents were found to significantly influence the mechanical properties of the polymer housing and adversely affect socket stress relaxation behavior. The properties of the polymer housing were found to be sensitive to temperature owing to its visco-elastic nature. Polymer housing relaxation was therefore identified as a principle contributor to failure in stamped metal sockets under high temperature environments.

In the latter part of the study, numerical modeling was used to develop a methodology for assessing socket life expectancy under temperature and deformation loads. A full visco-elastic characterization of the polymer housing was conducted and the measured properties were subsequently used to model socket stress relaxation time to failure.

The results of this study indicate that socket temperatures under electrical loading can be significantly higher than those called for by EIA test specifications for LGA sockets. Passing tests that are not stringent enough to account for worst case scenarios can pave the way for field failures. The methodology outlined in this dissertation may be used to determine socket temperature environments and their effect on socket life expectancy.

EFFECT OF JOULE HEATING ON THE RELIABILITY OF STAMPED METAL LAND GRID ARRAY SOCKETS

By

Vidyullatha Challa

Dissertation submitted to the Faculty of the Graduate School of the
University of Maryland, College Park, in partial fulfillment
of the requirements for the degree of
Doctor of Philosophy
2010

Advisory Committee:
Professor Michael Pecht, Chair
Dr. Michael Osterman
Dr. David McElfresh
Professor Patrick McCluskey
Professor Peter Sandborn
Professor Chris Davis

Dedication

To my mother Dr. Jayaparada Challa for all the sacrifices she made in single-handedly raising me and for teaching me never to give up;

To my father Dr. Upendra Challa (late) for being my inspiration;

To my husband Gopi Mandava for his unstinting love, rock solid support and constant encouragement;

To my daughter Navya Mandava for always putting a smile on my face;

To my former adviser Prof. Stephanie Lopina (late) for being a supermom, a super-researcher and for being a great role model;

And to all the friends and family who have stood by me through the ups and downs of the past few years.

Acknowledgements

I would like to thank my advisor Prof. Michael Pecht for his guidance through the years and for always encouraging me to do better; Dr. Michael Osterman for many discussions on my research, for reviewing all my work and for always being available to talk; Dr. David McElfresh from Oracle Corporation for being a mentor, and for the many hours spent on technical discussions and reviews; my committee members Prof. Patrick McClusky, Prof. Peter Sandborn and Prof. Chris Davis for their valuable feedback on my work. I would also like to thank Prof. Abhijit Dasgupta for extensive reviews and discussions on my work; Prof. Avram Bar-Cohen for discussions on the thermal aspects of my study, Dr. Michael Azarian for feedback on my work, Dr. Leon Lopez for reviewing my papers, Dr. Das for helping out on a range of technical, professional and personal issues and Dr. Changsoo Jang for discussions on visco-elastic modeling.

I would like to thank all my friends at CALCE for their support and friendship; Gayatri Cuddalorepetta for being a friend, critic and reviewer; Lyudmyla Panschenko Lei Nei, and Gayatri for sharing many a laugh and for all the good times; Pedro Quintero, Nishad Patil, Vikram Srinivas, Sandeep Menon, Gilbert Hadad, Mohamad Alam, Elviz George, Sony Mathew and Anshul Shristavastava for their friendship, support and help during my years at CALCE.

Table of Contents

List of Tables

List of Figures

Chapter 1: Introduction

Motivation

Performance requirements in high-end microprocessors have increased tremendously in the last decade, leading to higher I/O requirements and interconnect densities. A single electronic package can now house several microprocessor units known as cores, with I/O counts running into a few thousands. The number of cores in high-end microprocessors has been increasing in recent years, in an effort to meet greater performance requirements. The International Roadmap for Semiconductors (ITRS) projects the number of cores to increase 1.4 times per year for networking applications [1]. The required processing power is expected to increase 250 times in the next 15 years, and power consumption to increase five fold by 2022 for the non-portable electronics segment. Furthermore, interconnect densities have been increasing and pitch requirements have been getting smaller. As the electronics industry moves towards finer interconnect and pitch, higher processor temperatures and current densities, the reliability risks in high density socket applications due to Joule heating are expected to become increasingly important. The resulting higher temperatures can lead to stress relaxation, melting of the surrounding polymer, or thermal runaway conditions [2]. While the currents per pin used today and in the near future, are not high enough to cause contact or polymer melting or mass migration phenomena, they have the potential to adversely influence socket mechanical behavior during operation and lead to premature failure by stress relaxation. This

study investigates Joule heating and the influence of the resulting high temperature environments on the reliability of high density stamped metal land grid array sockets.

Land Grid Array Sockets

Higher I/O requirements in multi-core and multi-threaded processors, which call for the use of high density packages with large footrpints, present quality and reliability challenges for traditional solder joints. Soldering is the conventional method of attaching a microprocessor to the printed circuit board (PCB), creating a permanent connection that cannot be easily upgraded or repaired. As I/O requirements increase, leading to packages with larger footprints and higher densities, there is greater tendency for solder balls to crack over time, due to the coefficient of thermal expansion (CTE) mismatch between the electronic package and the PCB [3]. Furthermore, as I/O counts increase and pitch requirements decrease, achieving good quality solder joints during the manufacturing process becomes increasingly difficult. Inaccurate placement, coplanarity issues arising from warpage and non-uniformity of temperature profiles across the large package body contribute to the formation of imperfect solder joints. If failures do occur, it becomes difficult to rework these high density packages [3].

Land grid array (LGA) sockets [4][5][6] provide a separable, high density interconnect solution that eliminates the reliability and quality risks to the package associated with soldering. A socket, unlike permanent solder joints, facilitates microprocessor upgrade and repair at any time. The use of sockets also facilitates component test and burn-in and provides supply chain flexibility for instance, by

converting through hole components to surface mount or vice-versa [3].

An LGA socket consists of contacts embedded in a plastic housing that, by means of compression, form the electrical and mechanical connection between an LGA component and the PCB. An LGA component is similar to a ball grid array (BGA) component, with pads on the underside instead of solder balls. Use of LGA components in conjunction with sockets allows the use of large footprint packages with the ability to accommodate high I/O counts. A separable interposer that is able to move freely between the component and the PCB is better able to dissipate the strain due to CTE mismatch than solder joints [5].

LGA sockets are available in conductive elastomer, wire-wound and stamped metal designs [4][5][6]. In the elastomer design each contact button is made of an elastomer filled with conductive particles that make contact on compression. The wire-wound design uses contacts made of gold plated metal wire that is randomly wound into cylindrical buttons. Stamped metal designs use contacts that are stamped and formed, usually into a C or G shape (Figure 1).

While both the wire-wound and elastomer designs offer the advantage of multi-fold contact redundancy, or multiple electrical paths within a single contact, they also suffer from significant disadvantages. The wire-wound designs are approximately 2.5 - 5 times more expensive than stamped metal and elastomer sockets, making them a reliable but expensive solution. A significant disadvantage of the elastomer sockets is that their resistance behavior is highly sensitive to environmental changes, making intermittent failures more likely [7]. Stamped metal designs provide a lower cost solution compared to wire-wound sockets and

potentially a more reliable alternative to elastomer sockets, using contact materials that have a long history of reliable operation.

Stamped Metal Socket

The stamped metal socket under study (Figure 1A) has C-shaped contacts housed in a liquid crystal polymer (LCP) matrix that provides alignment features and physical protection during handling. The contacts are made of a copper beryllium alloy and are protected from environmental exposure by a Ni/Au finish. A nickel underplate layer between the base metal and the gold plating has been shown to protect the contact alloy from corrosion through any porosity in the gold layer [8]. A second reason for using a nickel underplate is to act as a diffusion barrier and prevent diffusion of the base metal through the gold layer with subsequent oxidation, which can pose reliability issues [9]. The gold layer is typically 30 microinches thick while the nickel barrier layer is 50-70 microinches thick. During assembly, the LGA socket is compressed between the microprocessor package on top and the PCB below using loading hardware that typically consists of a heat sink, a bolster plate, springs and screws. A typical socket loading assembly is illustrated in Figure 2.

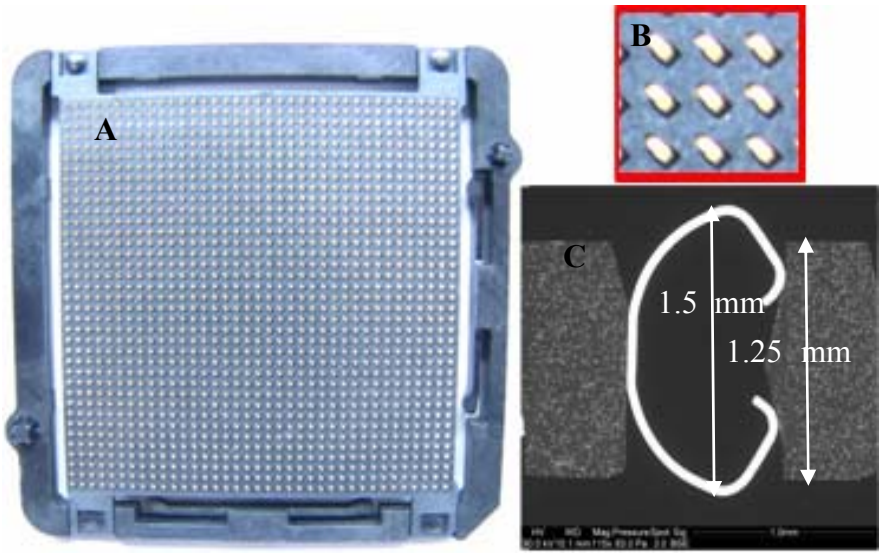

Figure 1: A: Stamped metal socket; B: Detail of contacts embedded in LCP housing; C: Cross section of a stamped metal contact

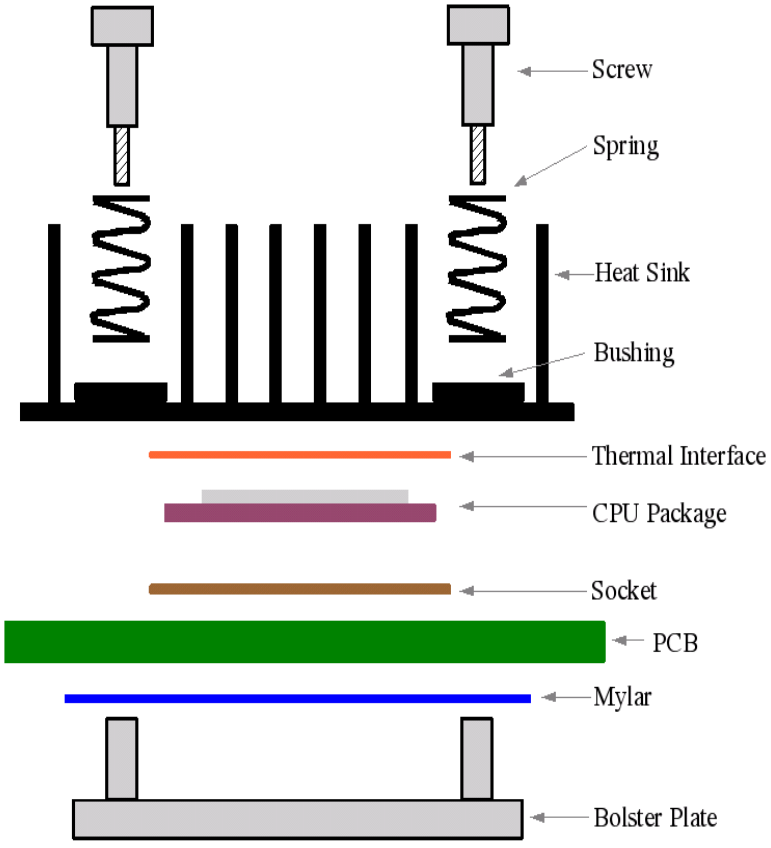

Figure 2: Typical LGA socket loading assembly

Problem Statement

The passage of current through the socket contacts results in temperature increases for both the socket contacts as well as the polymer housing. Higher currents through smaller interconnects can increase the risks of Joule heating in high-density socket applications, and accelerate temperature-dependant failure mechanisms such as stress relaxation. Copper beryllium alloys which have good stress relaxation resistance have been in use in connector applications for a few decades. However, due to the visco-elastic nature of the socket polymer housing, higher temperatures in the socket body can affect the mechanical properties of the polymer, leading to premature failure by stress relaxation. Stress relaxation which is the loss of force with time, results in an increase in contact resistance, and can eventually lead to failure in LGA sockets.

The current LGA socket standard (EIA 540BOAE) which recommends test conditions of 85 °C for 500 hours in order to assess the susceptibility to failure mechanisms under thermal aging, does not address Joule heating of socket contacts or the higher operating temperatures of current-day processors. Processors with operating temperatures close to 100 °C are already in use today. Higher temperatures from Joule heating can decrease life expectancy and result in unanticipated field failures. The LGA socket standard test conditions however are not tied to life expectancy and do not allow a calculation of acceleration factors. This may result in sockets that pass the LGA test specifications with subsequent field failures owing to higher temperature environments under electrical loading.

The objectives of this dissertation are to characterize socket temperatures during operation under electrical loading, to examine some of the factors that influence socket body temperatures and to provide a methodology that assesses the effects of these higher temperatures on socket mechanical behavior and socket life expectancy.

Overview of Dissertation

In the first part of this study the stress relaxation behavior of stamped metal LGA sockets was characterized under various temperature and compression conditions. Higher temperatures were found to increase the potential for premature socket failure by stress relaxation. Socket housing was identified as a principal contributor to failure in stamped metal LGA sockets under high temperature environments.

In the second part of this study, socket temperatures under electrical loading were characterized through a combination of experimental and numerical methods. Some factors that influence Joule heating including current, contact pitch, processor temperature and contact alloy were examined in order to determine their influence on the socket body temperatures driven by Joule heating. All of the factors were found to significantly influence the temperature rise driven by Joule heating, with the contact alloy and processor temperature having the most significant effects.

In the final part of this study, a methodology to assess stamped metal socket life expectancy under temperature and compressive loads was developed. Stress relaxation time to failure was modeled using numerical methods. Visco-elastic

behavior of the polymer housing was characterized, and the measured properties were used to model the behavior of the socket under time and temperature loading conditions. Time to failure predictions were obtained for upper and lower bounds of processor temperature and current per pin for power contacts. The results determined that standards based testing does not reflect the higher temperatures resulting from Joule heating, and the associated failure mechanisms. Joule heating is a reliability consideration that must be taken into account for high density sockets. Socket qualification testing must be conducted at higher temperatures that are reflective of electrical loading or with power to account for Joule heating effects.

Chapter 2: Literature Review

This chapter presents a literature review on LGA sockets, Joule heating in contacts/connectors, and stress relaxation in both contact alloys and polymers. The bulk of the literature on LGA sockets was found to be on elastomer and wire wound (also called fuzz button) sockets. While there are a few papers on metal contact sockets, these are on sockets that are soldered at the motherboard side and not fully separable. Characterization and reliability assessment of stamped metal LGA sockets was identified as a gap which this dissertation strives to fill.

Land Grid Array Sockets

Several references are available in literature that present an overview of LGA socket types, failure mechanisms, opportunities and challenges[1][4][5]. Production LGA sockets are commonly available in conductive elastomer, wire wound and stamped metal designs (Figure 3).

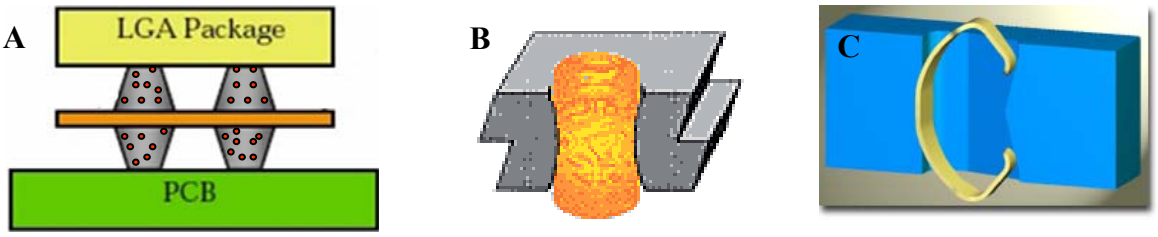

Figure 3 : Types of LGA Sockets, A: Metal in Elastomer Design, B: Wire Wound Design, C: Stamped Metal Design

Elastomer LGA Sockets

In the elastomer design each contact button is made of an elastomer, filled with conductive particles that make contact on compression or embedded with metal wires. Early work at IBM and AT & T investigated different designs of elastomer contacts such as pre-aligned particles within an elastomer matrix, curved and straight wires embedded in an elastomer matrix [10],[11],[12],[13]. The elastomer designs are extremely cost effective, offer contact redundancy and are easy to scale to a finer pitch.

Elastomer designs in general, however suffer from a host of reliability problems. Previous work at the CALCE research center on the metallized particle interconnect (MPI) design, which consists of silver particles randomly distributed in an elastomer matrix button, has shown that the elastomer is prone to stress relaxation (50% in 10 hours at room temperature) and creep [14]. Radial deformation of neighboring contacts was also observed to pose a shorting risk between adjacent contacts. Elastomer stiction which causes elastomer residue to be left on the pads or pad residues to adhere to the elastomer after disassembly was found to pose a further reliability risk. Resistance behavior was found to be extremely sensitive to temperature and cycling loading effects making intermittent behavior more likely [14]. In other work Liu *et al*. determined that contact resistance of MPI sockets was highly sensitive to temperature and force effects potentially impacting long term reliability [15]. Designs containing silver were found to be susceptible to electrochemical migration by Yang *et al*. [16]. A loss of surface insulation resistance was observed at 85°C/85% relative humidity (RH), 5 V conditions due to

electrochemical migration.

Yang *et al.* assessed the reliability of two kinds of elastomer sockets (MPI and Pariposer ball wires made of silver plated nickel beads) under mixed flowing gas (MFG) environments. Silver corrosion products were detected on both types of sockets while nickel corrosion products with whisker like growth were observed on the Parisposer designs. These whisker-like growths were found to pose a risk for shorting of contacts [17].

In other work, Yang *et al*. [18] analyzed creep and stress relaxation failure mechanisms with force and deformation-controlled assemblies. Creep, or time-dependent deformation, was found to range from 20 - 37% for temperatures in the range of 40 - 150 °C for 60-minute exposure. Stress relaxation reached 30 - 40% for temperatures between 40-125 º C.

Xie *et al*. [19] researched stiffness and stress relaxation behavior of elastomer socket contacts under mechanical load and temperature (10 to 100 grams, 26 to 183 ºC). Temperature increases were found to decrease button stiffness by 50% and stress relaxation of 50% was observed after 1 hour at 133 ºC.

The aforementioned elastomer socket literature evaluated sockets under short term conditions (<150 hours). Lopez *et al*. [20] characterized the long term behavior of elastomer sockets (2000 to 16,500 hours) under temperature environments and found that the resistance decreased over time. This decrease was attributed to an increase in a-spot area of the silver particles in the elastomer buttons over time. Other work by Lopez *et al*. [21] presents a methodology for monitoring elastomer sockets based on a physics of failure model and sequential probability ratio test.

Wire wound LGA Sockets

The wire wound design uses contacts made of gold plated metal wire that is randomly wound into cylindrical buttons. This design provides multiple points of contact, and offers good corrosion resistance and reliability [22],[23],[24][25]. However, this design requires high contact force per button which necessitates the use of expensive clamping hardware and also suffers from poor reproducibility. These designs are expensive and can be 2.5 to 5 times more expensive than stamped metal and elastomer sockets. Previous work at CALCE on this design studied the effect of wire diameter and button density on contact resistance [26].

Metal Semi-Separable Sockets

Several researchers have investigated semi-separable metal LGA sockets which are soldered at the motherboard side but offer a separable connection at the component side. Song *et al*. [28] demonstrated a numerical approach that was able to predict the maximum motherboard temperature based on the maximum allowable contact temperature for semi-separable metal LGA sockets. The correlation between contact interface temperature and motherboard temperature Tb were made at various combinations of Tb, package substrate temperature and contact current. Work by Tracy *et al.* discusses the fabrication process, process variables and reliability testing on a micro-spring based socket which is again soldered to the board [36]. Reliability testing included temperature life of 1000 hours at 105 °C, thermal cycling 1000 cycles from -55 to 125 °C.

Stamped Metal LGA Sockets

In the stamped metal design each contact is stamped and formed, usually into a C or G shape, with the contact behaving like a spring [37][38] . Contact redundancy is usually limited in stamped metal designs, with single or duals points of contact. This makes Joule heating a greater reliability risk for these specific types of sockets.

Work by Neidich describes the fabrication, product specification and reliability testing on a fully separable stamped metal socket as per EIA specification [37]. Datasheets summarize the specifications and qualification of two other fully separable stamped metal LGA sockets [39][40].

Investigation of Joule heating Connectors/Contacts

Several studies have determined the temperature rise due to the passage of current using experimental and analytical methods for various applications ranging from power connectors to micron sized wafer probes. Other researchers have explored failure mechanisms under elevated current. These include mass transport phenomena such as electromigration as well as mechanical phenomena such as stress relaxation. This section summaries some of the studies.

A thermo-electric analysis was conducted by Ahmad and Sitaraman to investigate Joule heating effects in micro-spring probes used for wafer-probing applications. ΔT values of around 93 °C above ambient were observed at the spring tip at maximum currents of 0.25 A. Contact resistance was not modeled in this study, but the bulk resistance was extremely large due to the small dimensions of the micro-springs (12 μ pitch) [29].

McGowan [30] conducted experimental and finite element analysis (FEA) investigations of Joule heating in power connectors and determined that ΔT values of upto 80 °C were reached at 40 A of current. It should be noted that these connectors have much larger dimensions than in work conducted by Ahmad *et al*. The temperature rise was found to be sensitive to airflow.

Xin *et al*. [31] conducted FEA and experimental investigations on separable power connectors and determined that maximum connector temperatures were 140 °C for 6W power and 380 °C for 14 W (above specification limits).

A familiar example of Joule heating in the electronics industry may be found in the fusing and arcing of tin whiskers [32][33]. Tin whiskers, which are filament-like structures that grow from tin-rich surfaces, have a bulk resistance that is in the tens of ohms depending on the diameter (usually less than 10 μm) and length (can be upto a few millimeters long). A 3 mm long whisker with a 2 micron diameter, for instance, has a bulk resistance of approximately 35 Ω. Joule heating effects in tin whiskers can cause the whiskers to fuse and melt below 50 milliamps [33]. Joule heating effects in whiskers can also cause metal vapor arcing under vacuum conditions. Therefore contacts or filaments with small dimensions (large aspect ratios) can result in large bulk resistances and therefore significant Joule heating effects. Various studies have determined that the temperature rise due to Joule heating, depends on a number of factors such as material properties, geometry, load, boundary conditions and electrical resistance.

Runde *et al*. [34] observed electromigration and subsequent contact degradation in aluminum contacts at current densities greater than 10^7 A/cm^2. Low

melting metals such as tin, lead, aluminum and zinc have greater propensity for electromigration when compared with higher melting point metals such as copper, gold and silver due to higher associated activation energies. Operating current densities in stamped metal LGA sockets are low enough that electromigration is not a concern.

Stress Relaxation in Copper Beryllium Contact Alloy

Copper beryllium alloys which contain less than 2% beryllium are typically used in electronics application because of their high strength, stress relaxation resistance and resistance to permanent set [35]. Fox *et al*. conducted stress relaxation tests on copper beryllium alloy strip and predicted the stress remaining after 40 years to be 80-90% for C17200 copper beryllium alloy based on a 2000 hour test, depending on the temper [41]. According to Shapiro *et al*. the stress remaining in C17200 alloy after 10,000 hours at 105 °C is 96% [42] The datasheet for the C17200 alloy used in the socket under study specifies the 1000 hour stress remaining at 150 °C to be close to 90%, and ~60% at 200 °C [43] . Therefore C17200 alloy has been shown to have good stress relaxation resistance and is unlikely to stress relax significantly at temperatures of less than 150 °C.

Stress Relaxation in Polymer Housing

Viscoelasticity in liquid crystal polymers has been noted as a distinct phenomenon by several researchers [44][46][47] . According to Gervat *et al*. thermotropic liquid crystal polymers can be modeled using a spectrum of relaxation constants because they exhibit a range of relaxation times [46]. Generalized Maxwell

models and a time temperature superposition approach have been used by other researchers to predict the stress relaxation behavior of liquid crystal polymers [46][47]. Shiva Kumar and Das used the Wiilim Landau Ferry (WLF) time temperature superposition approach on liquid crystal polymer blends [48].

Chae *et al.* characterized the visco-elasticity of epoxy mold compound for electronics applications using the generalized Maxwell model along with a time temperature superposition approach [49]. Therefore the liquid crystal polymer housing used in socket applications is likely to stress relax owing to its documented visco-elastic nature.

Summary and Conclusions from Literature Review

1. The bulk of LGA socket literature is on the characterization and reliability of elastomer sockets, followed by wire wound sockets. Some studies have characterized semi-separable stamped metal sockets which are attached to the board but provide a separable connection at the component side. Characterization and reliability assessment of stamped metal sockets was identified as a gap which this dissertation strives to fill.
2. Several researchers have examined Joule heating in various applications from wafer probes to power connectors. The results of these studies indicate that temperatures resulting from Joule heating depend on various factors such as material properties, geometry, load, thermal boundary conditions and electrical resistance.
3. Stress relaxation resistance of copper beryllium alloy C17200 has been shown

to be very good at temperatures below 150 °C. Therefore any stress relaxation observed in the socket under study is likely to come from the polymer housing.

4. Several studies have shown that liquid crystal polymers exhibit distinct visco-elasticity, and therefore the polymer housing in sockets is likely to be sensitive to temperature effects.

Chapter 3: Stress Relaxation in Stamped Metal Sockets

This chapter examines stress relaxation in stamped metal sockets under different load conditions. Higher temperatures, that can result from Joule heating of the socket contacts, were found to influence socket mechanical properties, potentially leading to earlier failure.

Stress Relaxation and Stamped Metal Sockets

Stress relaxation refers to a decrease in stress with time, under given constraint conditions and at a specified temperature [50]. Stress relaxation in LGA sockets can lead to a decrease in the normal force, increase the sensitivity to micro-motion, and reduce the contact area [51]. Loss of normal force (Fn) results in an increase in contact resistance (Rc), which can eventually lead to failure. This behavior is represented by the expression below

$$R_c = \frac{\rho}{2}\sqrt{\frac{\pi H}{F_n}} \tag{1}$$

where ρ is the electrical resistivity of the contact, and H is the hardness of the contact finish [76]. (A hardness value that measures indentation area such Knoop or Vicker's hardness may be used. Rockwell hardness that measures indentation depth cannot be used in equation 1.) Note that the above equation applies to noble finishes where the constriction resistance essentially represents the contact resistance. For non-noble finishes an additional film resistance has to be added to the constriction resistance in order to obtain the contact resistance (equation 2). The film resistance is attributed to

the presence of oxide or corrosion films formed on the non-noble contact finish.

$$R_c = \frac{\rho}{2}\sqrt{\frac{\pi H}{F_n}} + \frac{\rho_f}{F} dH \qquad (2)$$

where d is the film thickness and ρ_f the film electrical resistivity.

An increase in contact resistance can manifest itself as intermittent failures or as an open in a functional circuit. As per EIA 540BOAE specifications for LGA sockets [50], an increase in contact resistance of 20 milliohms or more is considered a failure.

A compressive force applied using the loading hardware (Figure 2) creates microscopic contact regions at the LGA interfaces, completing the electrical and mechanical connection between the PCB and the LGA component. Stress relaxation can disrupt the microscopic contact regions and increase the contact resistance, making contact failures and intermittent behavior more likely. Stress relaxation is accelerated by thermal aging environments, such as those seen in electronic systems like enterprise servers [53].

Experimental Study

Force-Strain Behavior

The force-strain behavior of the socket was characterized to determine the strain condition above which the polymer housing is loaded. For the evaluation, 4 mm × 4 mm socket samples were cut out, each with nine contacts, as shown in Figure 1B. Three samples, and therefore a total of 27 contacts were tested at each condition. A constant compressive deformation rate of 0.004 mm/sec was applied, and the force

vs. strain behavior was recorded. For the purposes of this study, strain is defined as the change in contact height as a fraction of the original unmated height and does not refer to the Von Mises or true strain in the contact.

When a small compressive force is applied to the socket, the contacts bear the entire load and reduce their height. If the load is high enough, the contacts are compressed to the same height as the LCP, and the load is shared by both the contacts and the LCP housing. Loading of the LCP housing is not desirable during operation because this can result in polymer cracking and crack propagation between neighboring contacts. Both of these scenarios can result in contact movement and compromise the electrical performance of the socket. Engaging the polymer can also shift the load distribution over the socket contact array, creating non-uniform loading.

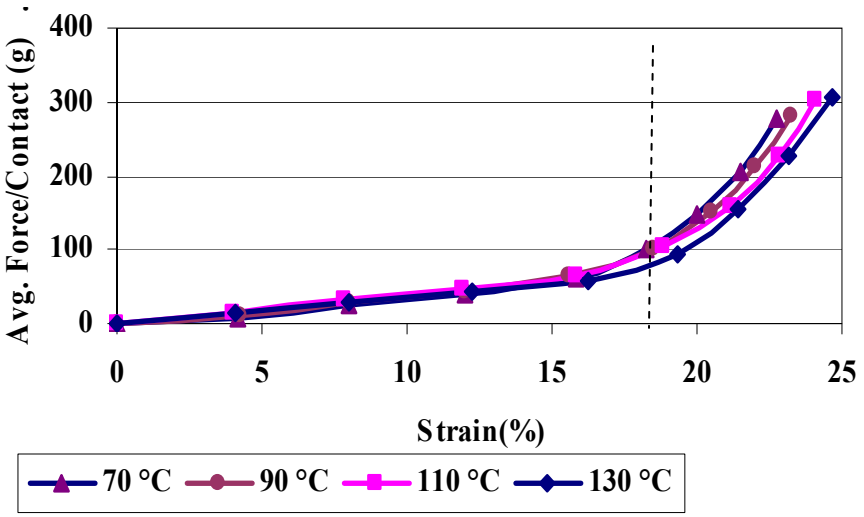

Figure 4: Force vs. strain behavior for stamped metal socket at different temperatures. Modulus transition occurs at approximately 17% compressive strain

Note that force was measured in this study rather than stress. If the polymer is engaged, the contact area is different from when the contacts carry the entire load,

and a stress representation would therefore be inaccurate. The force-strain behavior of the stamped metal socket was evaluated from 70 °C to 130 °C. The results depicted in Figure 4 show a low modulus (defined as force divided by strain for the purposes of this chapter) region followed by a transition to a higher modulus region at a compressive strain of approximately 17% (indicated by the dotted line in Figure 4). The modulus change may be explained by examining the height of the contact and the polymer housing. The height of the contact in the unmated state is 1.52 mm, while that of the polymer housing is 1.25 mm (Figure 1C). In the fully compressed state, the contact is compressed to the same height as the polymer (1.25 mm) and is therefore compressed to a strain of approximately 17%. Below the 17% transition value the C-shaped contact which behaves like a spring, and therefore has a low modulus, carries 100% of the applied load. Above the transition value, the contact and the LCP housing share the load. The rigid polymer dictates the overall strain behavior in this region and the system therefore exhibits a high modulus.

Notice that the force-strain behavior exhibits a more significant temperature dependence above the 17% transition point, with higher temperatures resulting in lower force values for a given strain. In other words, visco-elastic behavior is evident above the transition point, and this can be attributed to the polymer housing. The force-strain behavior highlights the fact that the socket body housing is sensitive to changes in temperature, and Joule heating effects from the contacts can change the mechanical behavior of the socket body.

Stress Relaxation Behavior

The stress relaxation tests included three strain conditions (10%, 15%, 20%) and four temperatures (70, 90, 110, 130 °C) for each strain condition. The 10% and 15% strain conditions were selected to represent nominal contact loading. The 20% strain condition was selected to represent an overload condition, with the polymer being engaged. The temperatures account for the nominal processor operating temperatures (70-100 °C for the configuration being studied), and for the Joule heating of the socket contacts. Each test was conducted for a duration of 3 hours.

The stress relaxation data for compressive strains of 10, 15 and 20% (Figure 5, Figure 6 and Figure 7) show that at higher temperatures a lower initial force is required to maintain the same compressive strain. For example, Figure 5 indicates an initial force of about 50 g at 130 °C, compared to 90 g at 70 °C for the same compressive strain of 20%. This is consistent with the fact that the polymer modulus decreases at higher temperatures and therefore requires less force to maintain a given deformation as illustrated in Figure 4. This is significant because higher temperatures associated with Joule heating can result in a lower normal force. A lower normal force increases the contact resistance and the propensity for failure by stress relaxation as indicated by equation 1.

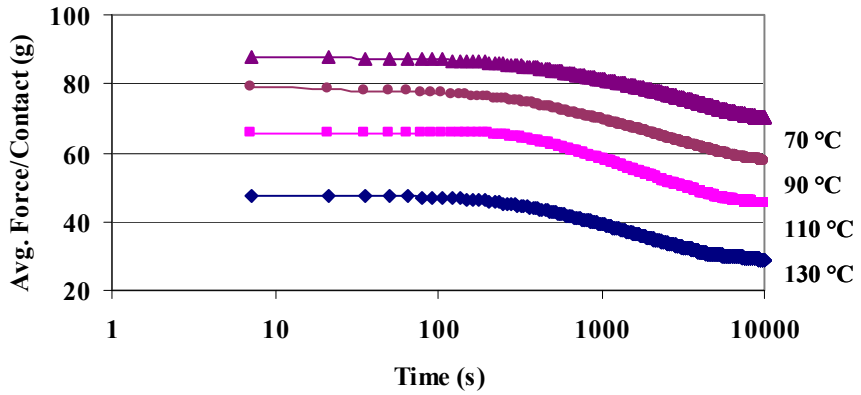

Figure 5: Force vs. time at 20% compressive strain

While Figure 4 indicates that stress relaxation occurred at 20% strain where the polymer is believed to be engaged, Figure 6 and Figure 7 show that stress relaxation also occurred at lower strains of 10 and 15% that represent cases where only the contacts were engaged.

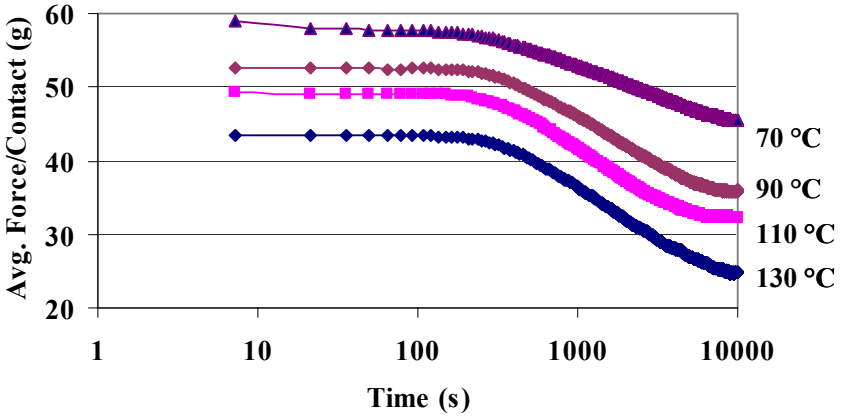

Figure 6: Force vs. time for 15% compressive strain

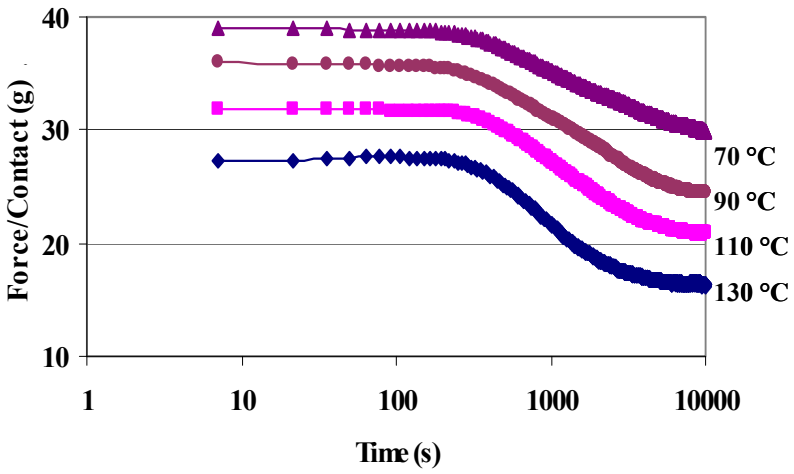

Figure 7: Force vs. time for 10% compressive strain

Discussion of Stress Relaxation Testing

When current flows through a socket contact it causes a temperature rise both in the contact and the surrounding polymer. Figure 5, Figure 6 and Figure 7 show that stress relaxation is strongly dependent on temperature with higher temperatures resulting in a lower normal force. Therefore, Joule heating of the socket contacts will lead to a lower normal force, potentially leading to premature failure by stress relaxation.

Stress relaxation was observed in the sockets both at 20% strain, when the polymer was believed to be engaged, and at 15% and 10% strains, when the contacts carried the entire load. Two arguments can be hypothesized here: 1) the contact alloy itself is stress relaxing; 2) the polymer is stress relaxing in the lateral direction, thereby contributing to stress relaxation in the longitudinal (Z) direction.

Stress relaxation may be considered as a manifestation of creep response under constraint [54]. Creep mechanisms are generally classified as diffusion based

and dislocation based [54]. Diffusion based creep in metals and metal alloys, becomes important at temperatures above 0.4Tm, where Tm is the absolute melting temperature. This value translates to 262 °C, based on a melting temperature of 1065 °C for copper beryllium alloy. Since the operating temperatures of 70-130 °C are well below this value, diffusion based creep effects from the contact alloy are likely to be small. Below 0.4Tm, creep can occur due to dislocation glide mechanisms which occur at intermediate temperatures and high stresses [54]. However for copper beryllium alloy these effects are small due to dislocation blocking from the multiphase structure of the alloy.

Stress relaxation is also dependent on the active stress at any given time, and increases with stress. Stress relaxation typically becomes a concern when the stress approaches the yield strength of the contact material. Design rules call for high yield strength of the contact alloy, so that operating stresses are well below the yield strength [5]. Therefore stress relaxation contribution from the contact alloy is likely to be small. At a given time, however it is possible that some contacts are under plastic deformation.

Several studies have confirmed that C17200 copper beryllium alloy has very good stress relaxation resistance, and can survive at least 1000 hours at 150 °C with 90 % remaining stress [41][42][43]. Relaxation observed experimentally in this study therefore has to be attributed to the polymer housing. However, stress relaxation was observed when the polymer was not being engaged in the longitudinal direction.

Therefore it was hypothesized that the polymer which is under constraint in the transverse direction is stress relaxing laterally, thereby taking less force to

maintain a specified deformation in the Z direction. This could explain the fact that relaxation was observed in the socket, even when the polymer was not loaded in the Z direction, represented by compressive strains of 15% and 10%. To test this hypothesis, small pieces of the polymer were tested for stress relaxation in the transverse direction. The polymer stress relaxed in the transverse direction to an average residual stress of 55% based on three samples (Figure 8). This hypothesis will be confirmed in chapter 5 through the use of finite element modeling.

The stress relaxation curves in Figure 5, Figure 6 and Figure 7 show an initial plateau region followed by a drop. This is consistent with visco-elastic models such as the generalized Maxwell models for polymers reported in literature [55][56]. In other words, the force-strain curve in Figure 4, as well as the stress relaxation curves in Figure 5, Figure 6 and Figure 7 suggest visco-elastic behavior of the polymer housing. The properties of the polymer housing therefore greatly influence the socket stress relaxation behavior.

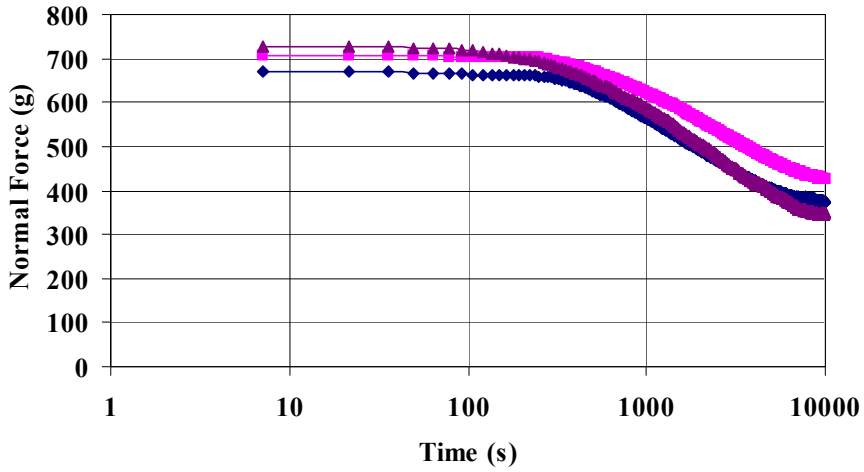

Figure 8: Force vs. Time plot of the polymer loaded in the transverse direction at 1% compressive strain at 130 °C

Electrical Resistance behavior

To determine the effect of stress relaxation on the electrical behavior of the socket, the resistance was measured as the normal force was varied, using a four-wire measurement method. The electrical resistance measured here comprises a bulk resistance and two contact resistances at each of the contact interfaces. The bulk resistance is not sensitive to force, and therefore any change in the total resistance due to stress relaxation may be attributed to a change in the contact resistance. The resistance measurements were made using the automated contact resistance probe [57][58] developed at the CALCE research center. The probe consists of a gold plated copper probe with a nickel underplate layer.

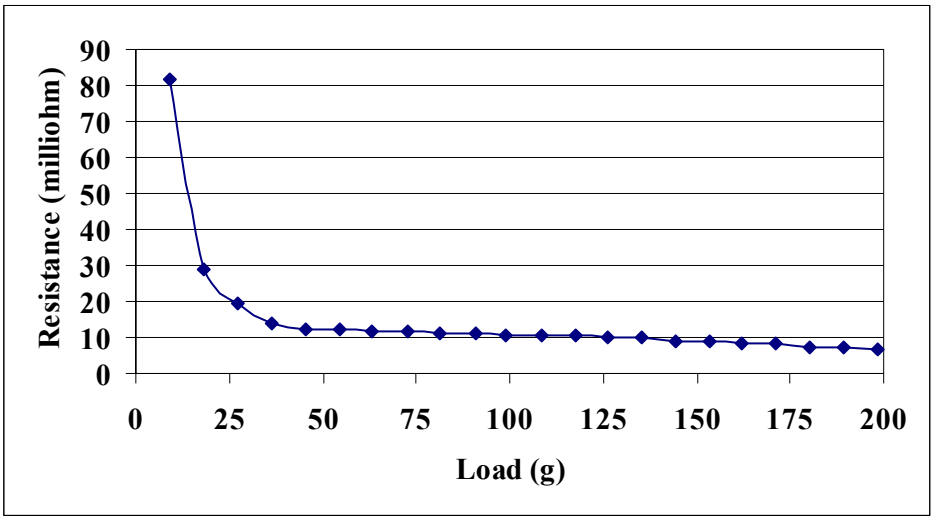

Figure 9: Contact resistance vs. force

The minimum normal force required to maintain a stable contact resistance is dependant on a variety of factors that are specific to the socket design. For the socket configuration used in this study, the results in Figure 9 show that above 50 g the

contact resistance is not very sensitive to changes in the normal force. Below a normal force of approximately 35 g/contact there is a sharp increase in contact resistance, for a small drop in the load. In this region the contact resistance exhibits a very high sensitivity to load, which would make failures more likely, especially if micro-motion or vibration effects are present. A representative temperature-force-resistance plot is illustrated in Figure 10.

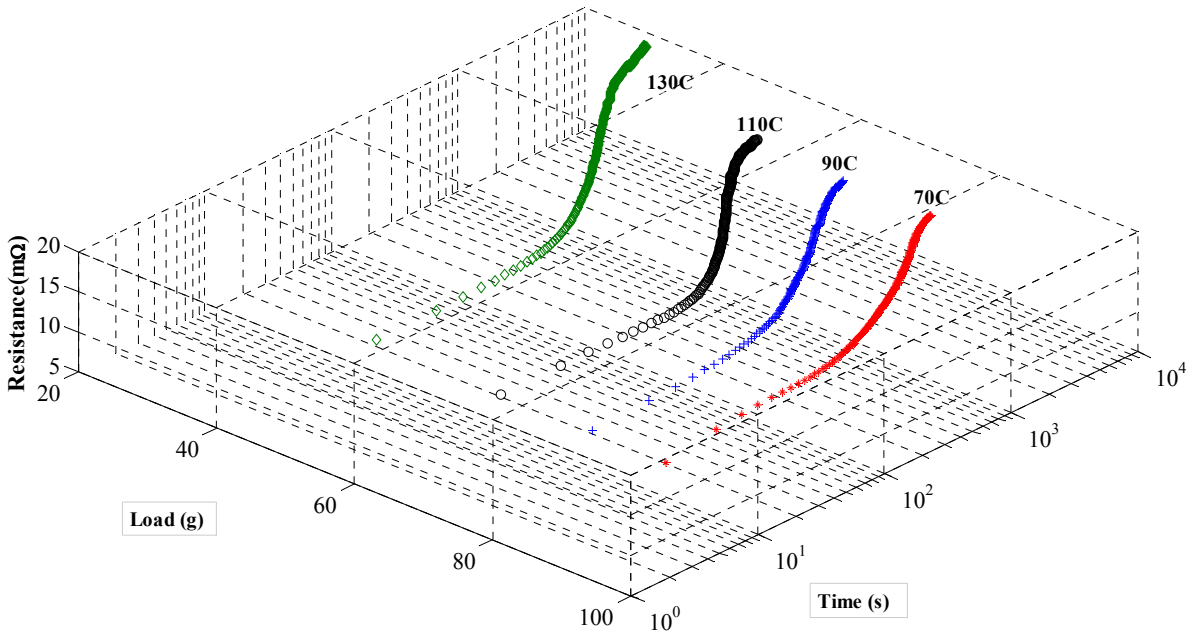

Figure 10: Representative Force-Temperature-Resistance Curve

Conclusions

In this study stress relaxation behavior of stamped metal sockets was investigated under temperature and compressive loads. Force-strain measurements of the stamped metal socket under study revealed distinct regions of contact loading vs. polymer engagement. Stress relaxation was observed not only when the polymer was engaged but also when the contacts carried the entire load. This behavior may be due

to lateral stress relaxation, which was confirmed experimentally on the polymer housing.

The electrical resistance behavior indicated that below a critical force, failure was more likely owing to the sensitivity of contact resistance to changes in force. Higher temperatures were found to result in a lower normal force, increasing the propensity for failure. Therefore higher temperatures resulting from Joule heating of the socket contacts, can increase the propensity for failure by stress relaxation.

In chapter 4, Joule heating is investigated as a function of current, as well geometry and material properties, through a combination of experimental and numerical methods. In chapter 5, a methodology that models time to stamped metal socket time to failure is presented. Stress relaxation is modeled using measured visco-elastic properties for the polymer housing and time to failure is determined at the temperatures resulting from Joule heating.

Chapter 4: Investigation of Joule Heating in Stamped Metal LGA Sockets

Introduction

As greater currents pass through the microprocessor interconnect, higher temperatures driven by Joule heating are expected to pose a reliability risk to high pin count microprocessor sockets. An investigation of stress relaxation in chapter 3 demonstrated that higher temperatures in the socket body can decrease the normal force, and increase the propensity for socket failure. In this chapter the factors that influence Joule heating in stamped metal sockets, potentially contributing to premature failure, are investigated.

Several researchers have characterized Joule heating for different applications ranging from wafer probes to power connectors [29][30][31]. However the results are not directly applicable to this study, because temperatures driven by Joule heating depend on various factors such as material properties, geometry, architectural parameters, load and thermal boundary conditions. An experimental investigation of all of these factors would involve a comprehensive test matrix, which can be time consuming and expensive. Therefore a combination of experimental and finite element analysis was used in this study to investigate the influence of material properties, boundary conditions, load and architectural parameters on Joule heating of stamped metal socket contacts.

The passage of current through the metal contacts results in higher temperatures for both the metal contacts as well as the socket housing. Estimating socket temperatures under electrical loading can help original equipment manufacturers (OEMs) and socket manufacturers to test for and mitigate the risks from temperature-related failure mechanisms. These temperature values may be used to determine socket mechanical properties during operation. Higher temperatures associated with Joule heating of socket contacts also have implications on qualification test conditions. Temperatures higher than nominal processor temperatures need to be used in socket qualification to account for worst case temperatures (in view of Joule heating effects) in order to avoid field failures.

A parametric study, using finite element analysis, examined the effect of varying the contact pitch, microprocessor temperature and the contact alloy properties on the socket body temperatures due to Joule heating. The effect of varying each of the three parameters was found to be statistically significant with the contact alloy properties and processor temperature being the most important. Choice of contact alloy and efficient thermal management are therefore key to mitigating Joule heating and the associated reliability risks in stamped metal LGA sockets.

Joule Heating in Stamped Metal LGA Sockets

The temperature of socket contacts (and housing) during operation is influenced by a number of factors, such as current, electrical resistance, thermal boundary conditions, material properties and socket configuration. Temperatures of high-end microprocessors can range from 70 to 100 °C, owing to self heating during

operation. In addition, as current flows through the socket contacts heat is generated, resulting in temperature increases for both the contacts and socket housing. Of the total heat produced, a fraction is lost to the surrounding environment while the remainder contributes to socket temperature rise. Socket final temperatures result from the heat balance between the Joule heat generated by the current flow and the heat dissipated to the surroundings.

The Joule heat produced in the socket is a function of current and resistance, and is given by I^2R. The total resistance is comprised of bulk and contact resistances. The bulk resistance is influenced by geometry and material properties (Equation 2), while the contact resistance is influenced by contact finish and normal force (Equation 1).

$$R_b = \frac{\rho}{A} l \tag{3}$$

Contact resistance is influenced by contact finish and normal force (Equation 1).

$$R_c = \frac{\rho}{2}\sqrt{\frac{\pi H}{F_n}} \tag{1}$$

The normal force in this study was high enough that the resistance was insensitive to force, and was therefore not a factor in this investigation. This is illustrated in Figure 9, above a normal force of approximately 50 g, where the resistance is fairly constant.

Some of the Joule heat produced is lost to the surroundings through conduction and convection. Heat loss is dictated by thermal boundary conditions, material properties of the contact alloy and surrounding materials, as well as the architectural parameters. Therefore, an FEA model was developed to assess the

effects of current, processor temperature, contact pitch, and contact alloy properties on the socket temperature during operation.

Approach

A combination of experimental and finite element analysis was used to determine the temperature rise driven by Joule heating. The experiments were used to validate the FEA results. Numerical modeling allowed a parametric study to be conducted that investigated the effect of varying material properties, architectural features and boundary conditions. Further the FEA was able to provide an estimate of the contact alloy temperature, which is difficult to measure experimentally owing to the small dimensions ands inaccessibility of the contact.

Experimental set-up

The experimental set-up is illustrated in Figure 11. Socket samples with a single contact was cut out and compressed between two copper disks. The disks were plated with 30 microinches gold over 50 microinches nickel to simulate the contact interfaces of a real LGA assembly. The upper disk was attached to the loading plate of a compression tester and a force of 130 g was used in order to ensure full compression. Based on the force-resistance curve of Figure 9, this force is high enough that resistance if fairly constant. The lower disk was attached to a hot plate in order to simulate the presence of a powered microprocessor with a maximum operating temperature of 100 °C. Double-sided Kapton tape attached to the non-contacting surfaces of the copper disks was used to electrically isolate the contact system from the rest of the set-up.

A 3 mil wire thermocouple, with nominal bead size of twice the wire diameter, was attached to the socket housing using slivers of kapton tape. Before installation, the thermocouple accuracy was verified by measuring the temperature of an ice water bath as well as boiling water, and no calibration was found to be necessary. The experiment was conducted at room temperature ambient conditions. The contact was powered on after steady state temperature conditions were reached and temperature and resistance were measured.

The temperature rise on the polymer housing (driven by Joule heating) was experimentally measured next to the powered contact (Figure 11) for currents of 1, 2 and 3 A.

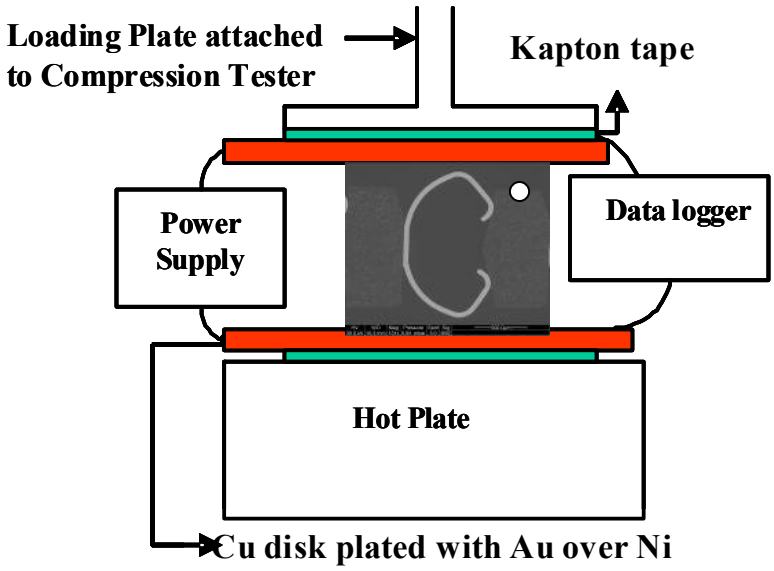

Figure 11: Experimental set-up consisting of a compression tester, power supply for applying the current and a data logger for measuring voltage drop. Dot indicates thermocouple location. Figure not to scale.

FEA Model Parameters and Properties

Commercial FEA software ANSYS was used to model the thermo-electric behavior of the LGA socket under a range of currents, and to conduct a parametric study. Current values ranging from 1-3 A were investigated in this study. Power contacts in high end computer systems carry an average of 1.5-2 A, with 3 A used as the worst case scenario. For the socket configuration under study, the maximum rated current is 3 A per contact. Signal contacts used in high end computer systems typically carry 200-300 mA current and do not experience significant Joule heating.

The metal contact, socket housing, and loading plates were modeled using the material properties of C17200 Copper-Beryllium alloy, 30% glass filled liquid crystal polymer, and copper respectively. The mechanical response of the materials was modeled using linear elasticity, in order to simulate compression of the socket. The structural material properties considered include modulus E, and Poisson's ratio ν. The thermal material properties considered were electrical resistivity and thermal conductivity. The materials and respective properties are provided in Table 1.

Table 1: Material Properties for Thermo-electric analysis

Material	Young's Modulus (GPa)	Poisson's Ratio	Electrical Resistivity (ohm-cm)	Thermal Conductivity (W/mK)
Cu-Be Contact alloy	125	0.3	7e-6	115
Copper Plates	125	0.3	1.7e-6	400
Polymer housing	15	0.38	1e12	0.5

Contact elements were modeled in order to represent the material interfaces between the polymer housing and contact alloy, as well as between the socket and compressing plates. The thermal contact conductance in ANSYS [59][60] represents a thermal contact resistance due to imperfect conduction across a contact interface (resulting in a temperature gradient at a contact interface), and has the same units as a heat transfer coefficient of W/m^2K. The contact resistance at an interface arises due to the presence of micro-roughness, leading to asperities (also called A-spots) contacting at only a small fraction of the apparent contact area. Heat (and current) is constrained to flow through these tiny asperities resulting in an additional resistance and temperature gradient across a contact interface. The contact conductance is expressed by the equation

$$q = hA\Delta T \tag{4}$$

where q is the heat flow (W), A the nominal contact area, h the contact conductance and ΔT the temperature gradient [61]. For this FEA analysis thermal conductance values of 16,000 W/m^2K and 3,000 W/m^2K were used to represent copper-copper and polymer-copper interfaces which are in the range reported in literature [61]. Analytical estimates of the thermal conductance for the metal-metal interface calculated as a function of the hardness of the surface finish as well as the nominal contact pressure, predicted a contact conductance of 18,500 W/m^2K for the metal-metal contact interfaces [62]. The analytical models used to calculate the thermal contact conductance are described in appendix 2. The model was relatively

insensitive to changes in polymer-metal contact conductance within the range reported in literature [61]. A value of 16,000 W/m^2K was able to match experimental data.

The experimental thermal boundary conditions in the experimental setup are captured in the FE model using isothermal temperature settings of 70 and 100 °C for the lower copper block to simulate the upper and lower bounds of processor temperature. The upper copper block was exposed to air with natural convection at 25 °C. Default adiabatic conditions were used otherwise.

Two-dimensional, plane stress analysis was used in the FEA analysis. The 2D element used for thermo-electric analysis in the contact alloy cannot model thickness. The out-plane thickness of each component was hence captured by modifying the resistivity (by dividing with thickness) and thermal conductivity (by multiplying with thickness).

Quadrilateral elements with mid-sided nodes were used and the model comprised of 962 elements and 2621 nodes. A mesh optimization study was conducted and going to a finer mesh increased the maximum temperatures by 5% while doubling the number of elements and the computational time. The coarser mesh was selected in order to reduce model complexity without significantly sacrificing accuracy. The mesh density is illustrated in Figure 12, where the unit cell of the socket is shown in the compressed state. The initial unmated state is depicted in Figure 13.

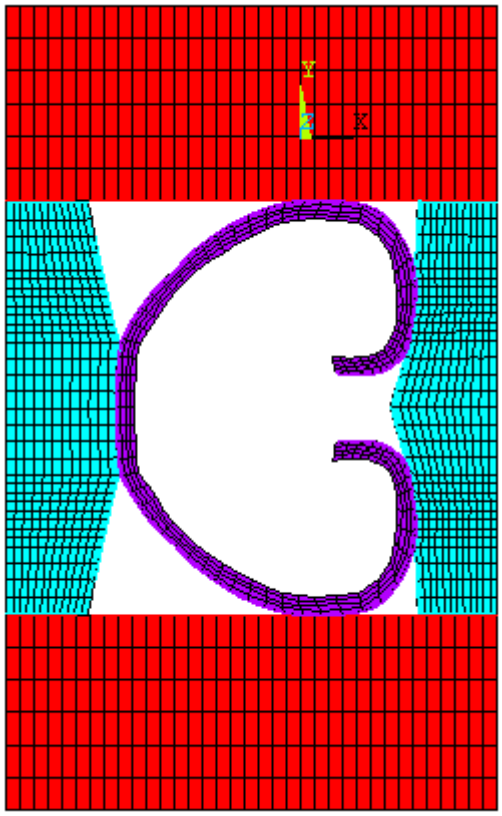

Figure 12: Mesh Density and Materials; C shaped structure is contact alloy, side walls are polymer housing, top and bottom plates are copper

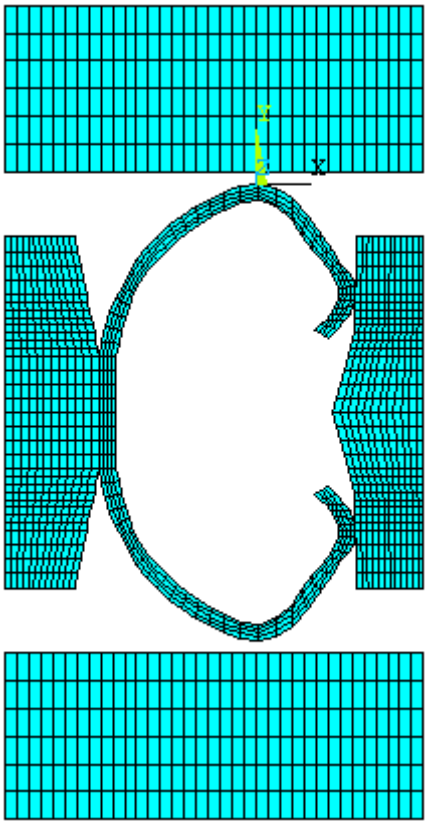

Figure 13: Model illustrating initial unmated state with compression plates not contacting the socket

Results and Discussion

Experimental Temperature Rise Associated with Joule Heating of Socket Contacts

Experimental results in Figure 14 show that, when the maximum rated current of 3 A was passed through a single contact (at a simulated processor temperature of 100 °C), the temperature of the LCP housing increased by ~40 °C. The contact resistance was determined to be 10 milliohms for the duration of the experiment. Note that the LCP housing temperature was 90 °C before the contact was powered, and 130 °C after power on at ~1000 s (a ΔT of 40 °C). This demonstrates that Joule heating of

the socket contacts causes the observed temperature rise. For currents of 2 and 1 A, a ΔT of ~ 20 and 10 °C respectively were observed.

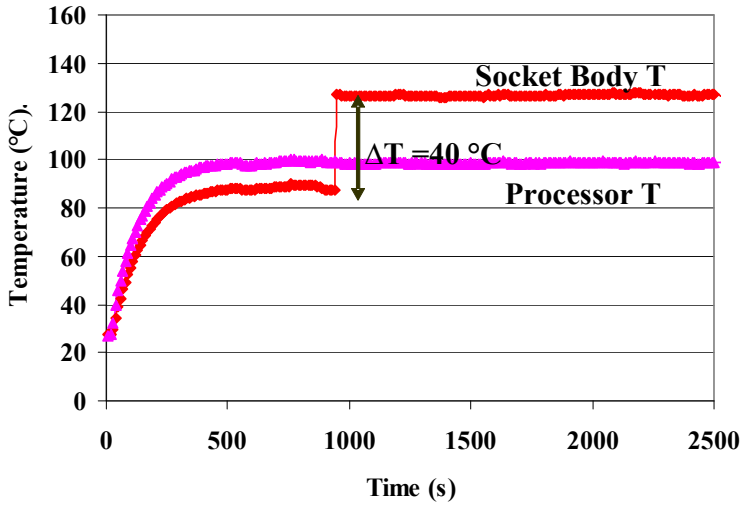

Figure 14: Illustration of temperature rise on powering up a single socket contact at ~1000s with 3A and 100 °C processor temperature

Finite Element Model: Contact Resistance vs. Bulk Resistance

The total electrical resistance for the contact alloy is comprised of a bulk resistance and two contact resistances at each of the two metal-metal contact interfaces. The bulk resistance is computed based on the geometry and electrical resistivity as

$$R_b = \frac{\rho}{A} l \qquad (3)$$

where ρ is the electrical resistivity, l is the length, and A is the cross sectional area. An analytical estimate, based on an equivalent length of the C-shaped contact, with electrical resistivity of C17200 Cu-Be alloy as 7 micro-ohm cm [64], indicated the bulk resistance to be approximately 8 mΩ. Using equation 1, the contact resistance

was estimated to be approximately 1 mΩ. The total electrical resistance is approximately 10 mΩ, and this was confirmed by using the experiment.

Both the bulk and contact resistances were incorporated into the FEA model. In order to determine the distributed self heating, the model uses the bulk resistance of the contact alloy segment through which there is current flow. The current path is indicated by the dotted line in Figure 15 . In order to incorporate heating from the interface resistance, a power input I^2R_c (Figure 15) was used at the top and bottom contact interfaces, where the 1 milliohm estimate was used for the contact resistance, R_c.

The FEA results indicated a significant temperature rise in the socket at 3 A current and 100 °C processor temperature (Figure 15). The average polymer housing temperature from the FEA model was 125 °C, while the average contact alloy temperature was 139 °C (The average temperatures for the contact alloy and the polymer housing were obtained by averaging out all the nodal temperatures for each material type). The spine of the C-shaped contact exhibited the highest temperatures due to resistive heating (resulting from the bulk resistance), since this region which is adjacent to the insulating polymer housing, is unable to effectively dissipate heat. Likewise the highest polymer temperatures are exhibited by regions of the housing that are in contact with the spine of the C-shaped contact. Polymer regions that are in contact with the open ends of the C, show lower temperatures. The interface heating is in regions that are able to effectively dissipate heat and therefore these regions are relatively cooler.

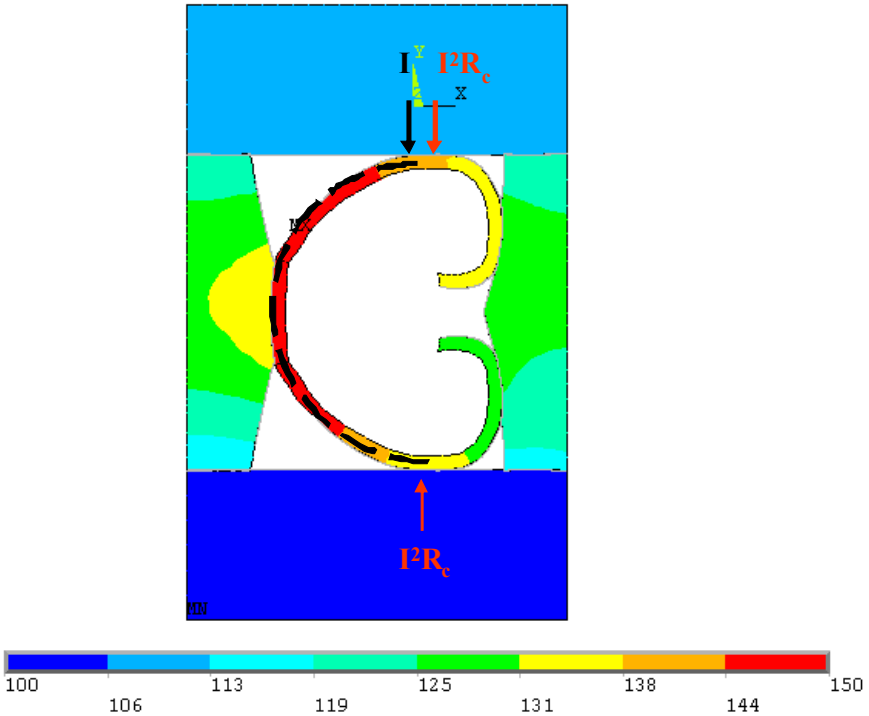

Figure 15: FEA results at 3A and 100 C "processor temperature".

Validation of FEA Model Results

The FEA model estimated the temperature at the thermocouple location to be 125 °C, while the experimentally measured temperature was 127 °C at 3 A current and 100 °C processor temperature. The model results also provided agreement with experimental results at 1 and 2 A (Table 2).

Table 2: Experimental vs. Model Results

Current (A)	Temperature Experimental (°C)	Temperature Model (at thermocouple location °C)
1	97	95
2	107	106
3	127	125

In order to qualitatively verify the temperature distribution, overstress currents of greater than 7.5 A (current at which melting was first observed, (Figure 16) were applied experimentally, and the samples were examined using scanning electron microscopy to identify the regions with the most thermally induced damage. The melting temperature of the polymer housing was determined to be 320 °C using differential scanning calorimetry (Appendix 1). Physical evidence showed that in every case, the polymer housing in contact with the back of the C shaped contact showed the most severe damage compared to the polymer region adjacent to the open ends of the C contact. Representative images showing thermally induced polymer melting due to overstress currents are illustrated in Figure 17 and Figure 18, while a pristine contact that did not pass current is illustrated in Figure 19. The temperature distribution illustrated by the model in Figure 15 therefore agrees with the physical evidence.

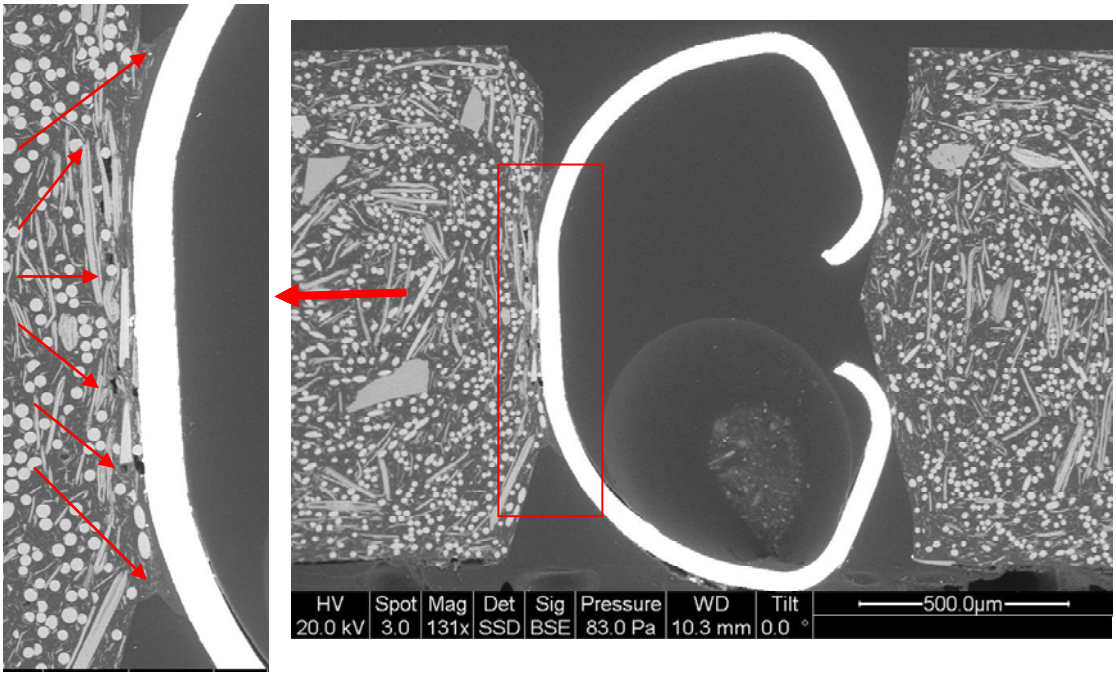

Figure 16: Scanning electron microscope image of sample that passed 7.5 A of current indicating polymer melting and voiding at spine of the C contact

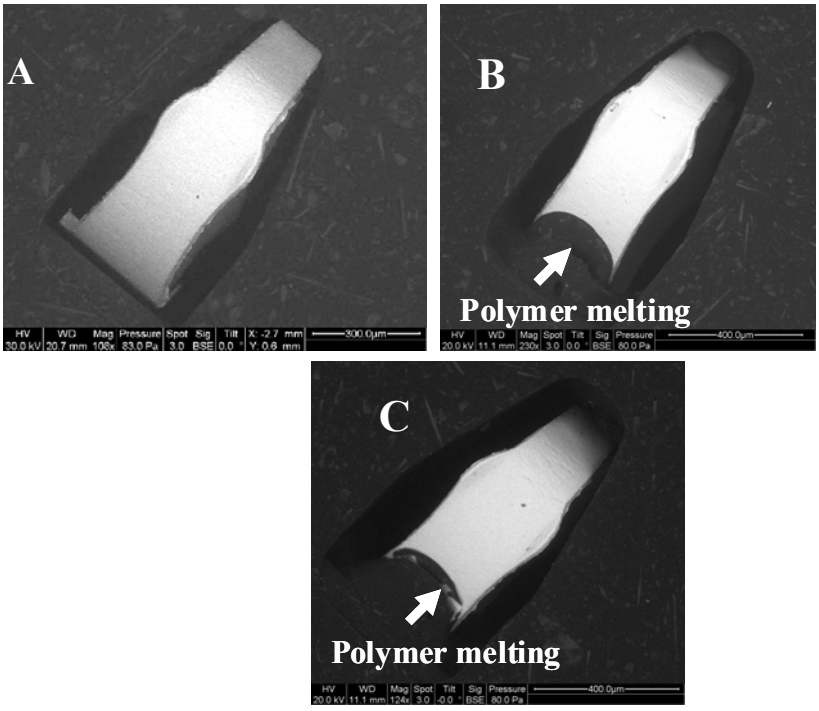

Figure 17: A. Pristine contact; B. Top side image of contact that passed 8.5 A; C. Bottom side image of contact that passed 8.5 A indicating thermally induced polymer melting at closed end of the C contact

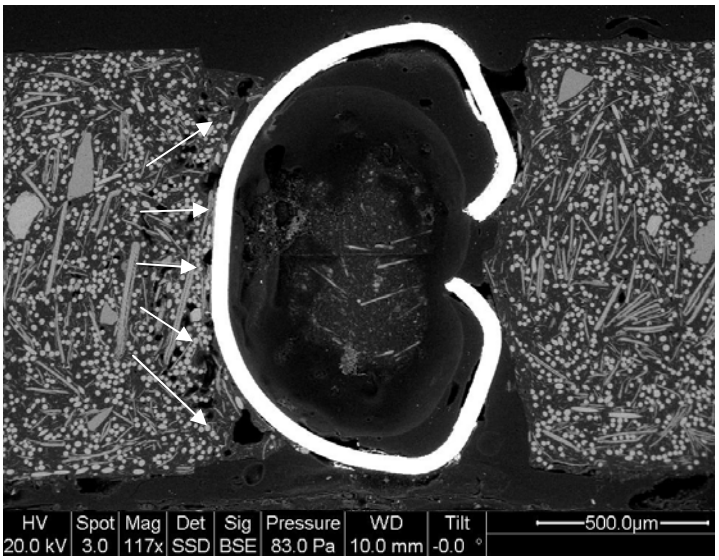

Figure 18: Cross section E-SEM image of sample that passed 8.5 A of current with arrows indicating polymer melting at the closed end of the C-shaped contact

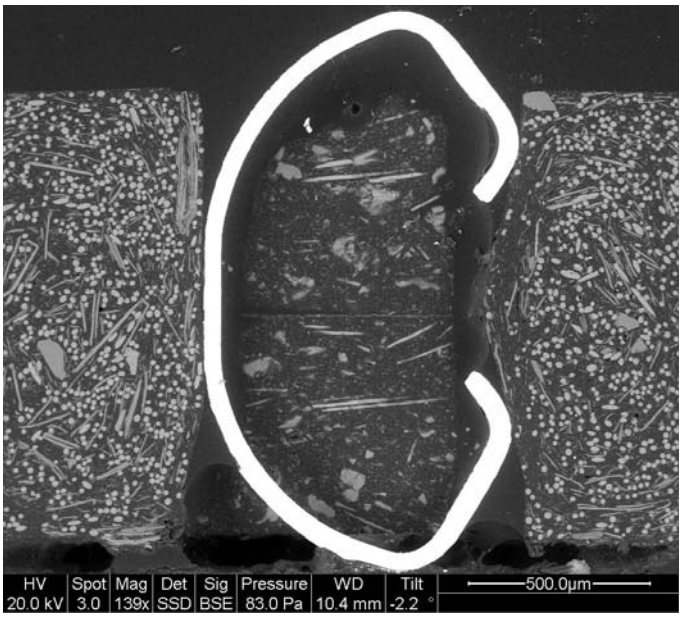

Figure 19: Cross section E-SEM image of Pristine Contact

Modeling Socket Temperature as a Function of Current

The average polymer and contact temperatures determined by the FEA for currents ranging from 1 to 3 A are listed in Table 3. The average nodal temperature for the polymer housing was computed using all the nodal temperatures for the polymer. The average contact nodal temperatures were determined in a similar manner. At currents of 1 A or less, and for a simulated processor temperature of 100 °C, the temperature rise when compared to the unpowered state was found to be less than 10 °C. At higher currents the temperature rise is large enough to have a significant influence on the polymer mechanical properties.

Table 3: Polymer and contact alloy temperature as a function of current through socket contacts for 100 °C processor temperature

Current (A)	Avg. Polymer Temp. (°C)	Avg. Contact Temp. (°C)
0	90	90
1	94	99
2	108	114
3	125	139

The socket studied in this research is typically sandwiched between a ceramic LGA package (attached to a heat sink) at the top and the PCB below, and is not in the primary heat transfer path between the microprocessor chip and the ambient. The back of the processor which is in contact with the socket is at a temperature that is approximately 10-20°C lower. Assuming a worst case temperature of 90 °C for the socket (100 °C processor temperature), when the maximum rated current of 3 A is passed through a contact, the temperature monitored at the socket body was found to increase by approximately 40 °C experimentally. Therefore, Joule heating of the socket contacts can result in worst case socket body temperatures of approximately 130 °C for the stamped metal socket being studied. Temperature environments in the powered state can be more severe than in the unpowered state, a fact that must be taken into account when conducting reliability tests.

The stress relaxation test results in chapter 3 have shown that a 40 °C rise in socket temperature (based on initial temperature of 90 °C) can cause an average drop in the contact normal force by 26%. A drop in the normal force leads to an increase in contact resistance. Higher socket housing temperatures, as a result of Joule heating of the contacts, can therefore increase the propensity for failure by stress relaxation.

Effect of Contact Pitch, Processor Temperature and Contact Alloy on Joule Heating of Socket Contacts

To determine the influence of contact pitch, choice of contact alloy, and processor temperature on the average socket housing (polymer) temperature during operation, a full factorial statistical design of experiments (DOE) was conducted using finite element analysis. Two levels were used for each of the parameters: contact pitch of 1 and 0.5 mm, processor temperatures of 70 and 100 °C, and contact alloys C17200 and C17460. A contact pitch of 1 mm was used to represent current LGA socket designs, while 0.5 mm was used in consideration of trends towards decreasing pitch sizes. The current was kept constant at 3 A.

The results from the DOE obtained through finite element analysis are presented in Table 4 and visually represented in Figure 20. The effects of all three parameters were found to be significant, with the processor temperature being the most significant, as shown in the half-normal plot of Figure 20 [67]. The half-normal plot is a visual method to determine significant parameters [68], and Figure 20 shows that the main effects are high when compared with the interactions. A main effect is the average effect of a single variable, while an interaction effect is the effect of a

factor averaged over another factor. The insignificant (i.e. near zero) effects lie close to zero and on a straight line, while the important effects fall off the line and are well displaced from zero [66]. Details on full factorial design and half normal plot concepts may be found in textbooks such as Wu and Hamada [67], while open source statistical packages such as R software may be used to generate half normal plots [68].

Table 4: Effect of varying processor temperature, pitch and contact alloy on polymer housing temperature through FEA

Processor Temp.(°C)	Pitch (mm)	Contact Alloy	Avg. Polymer Temp. (°C)
100	1	C17200	125
70	1	C17200	103
100	0.5	C17200	137
70	0.5	C17200	114
100	0.5	C174600	111
100	1	C174600	105
70	1	C17460	82
70	0.5	C17460	88

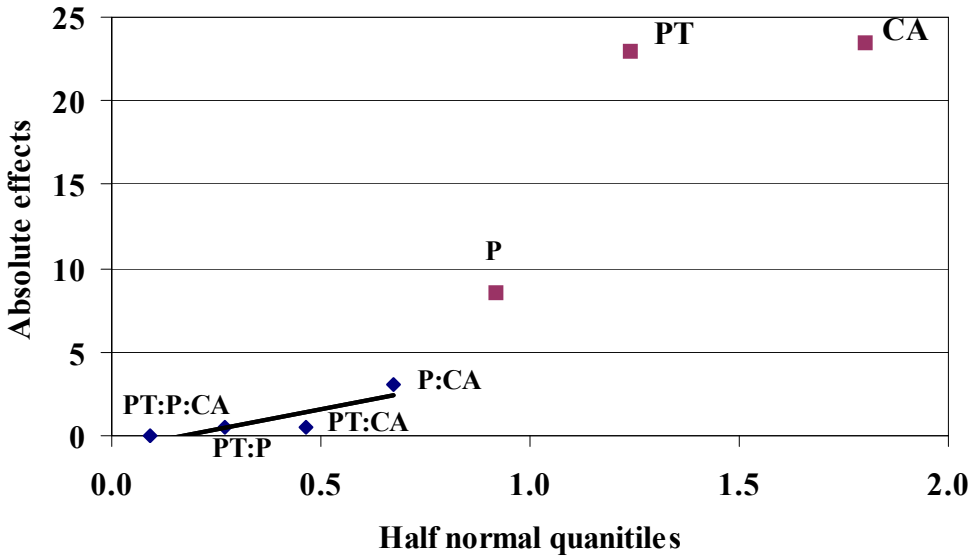

Figure 20: Determining significant parameters; PT: processor temp, P: pitch, CA: contact alloy; P: PT, PT: CA, P: CA and P: CA: PT are interactions of parameters. The main effects are significant when compared to the interactions (near zero effects that fall on a straight line) and fall off the straight line.

The pitch in the FEA model was varied by scaling the polymer width as well as the out of plane thickness. Decreasing the pitch from the standard 1 mm to 0.5 mm resulted in a 9% increase in polymer temperature. This is because the Joule heat sources are placed in closer proximity and there is less material in between to conduct away the heat.

The FEA results indicate higher temperatures associated with Joule heating of socket contacts, as the processor temperature increases. Reducing the processor temperature from 100 to 70 °C resulted in a 19% drop in the average polymer temperature. Efficient thermal management is therefore critical in order to minimize Joule heating of the socket contacts.

The commonly used contact alloys for stamped metal sockets include the

copper beryllium alloys C17200 and C17460. C17200 is a high strength alloy when compared to C17460 and this allows contact deflection without permanent set over multiple insertions [5][65]. A permanent set causes subsequent insertions to generate less contact deflection resulting in a lower contact force and higher contact resistance. A high resistance to permanent set also offers a larger working range in terms of contact deflection and therefore better accommodates flatness variations in the LGA package. C17460 on the other hand has better thermo-electric properties with higher thermal conductivity and lower electrical resistivity, and is therefore used in applications that require minimal Joule heating [65][43]. The compositions of the two copper beryllium alloys are presented in Table 5 and the thermo-electric properties used in the finite element model are listed in Table 6.

Table 5: Composition of C17200 and C17460 Copper Beryllium Alloys

Copper Beryllium Alloy	C17200	C17400
Composition	• 1.8 -2% Be • Other elements 0.2 % Si, Al, and 0.2 - 0.6 % Ni+Co • Balance Cu	• 0.15-0.5 Be • 1-1.4 Ni • Balance Cu

Table 6: Thermo-electric properties of C17200 and C17460

Contact Alloy	Thermal Conductivity (W/mK)	Resistivity (micro-ohm cm)
C17200	115	7
C17460	235	3.5

The FEA results indicate that changing from C17200 to C17460 alloy leads to a 20% drop in the average polymer temperature. This was attributed to an increase in thermal conductivity, as well as a decrease in electrical resistivity. As microprocessors move towards higher current densities in the future, Joule heating will be of greater concern. Selecting the right contact alloy with an appropriate balance between the mechanical and thermal properties becomes more critical as a consequence. Over the next few years as the current per contact increases, C17460 may not satisfy the conductivity requirements for minimal Joule heating, and new alloys may have to be explored.

Discussion

Contacts used in LGA sockets may be broadly classified as power/ground and signal contacts, based on the currents that they carry. Signal contacts used in high end computer systems typically carry 200-300 mA of current. Based on the results of Table 3, the signal contacts are not a significant source of Joule heating. The power/ground contacts in LGA sockets used for server applications can carry currents greater than 1A, with 3 A as a worst case scenario. The power/ground contacts can

experience significant Joule heating at higher currents based on the results in this study. The associated temperature rise can adversely influence the mechanical properties of the polymer housing and stress relaxation behavior of the socket.

While both the contact alloy and the polymer housing can experience a significant temperature rise due to the passage of current, the temperatures in the contact alloy are still low enough that stress relaxation in the contact alloy is considered insignificant. As described in chapter 3, creep effects typically become important in metals at temperatures above 0.5 Tm, where Tm is the absolute melting temperature. Based on a melting temperature of 1065 °C for copper beryllium alloy, 0.4 Tm translates to 265 °C. Therefore at worst case conditions of 3 A and 100 °C processor temperature, the average contact temperature (139 and 147 °C respectively for 1 mm and 0.5 mm pitch respectively) is well below 0.4 Tm. The polymer housing on the other hand is a visco-elastic material, and its mechanical properties will be influenced by a temperature rise. Higher temperatures cause the polymer modulus to decrease resulting in a lower normal force for a given deflection. This can lead to an increase in contact resistance resulting in premature failure.

This study shows that socket temperatures significantly higher than nominal processor temperatures can be reached depending on the electrical current that passes through the contacts. If qualification testing is to consider the most severe conditions in order to rule out field failures, Joule heating must be factored into socket testing. For instance based on a maximum processor temperatures of 100 °C, at 3 A maximum rated current, testing should be conducted close to 130 °C in order to account for worst case scenarios. The EIA LGA socket specification (540BOAE)

recommends high temperature life testing at 85 °C in the unpowered state in order to assess susceptibility to temperature-related failure mechanisms [52]. The temperatures recommended in the LGA socket specification are not high enough to reflect worst case processor temperatures in use today (greater than 100 °C [70]). Furthermore, as demonstrated in this study Joule heating due to the passage of current through the socket contacts, can cause an additional temperature rise and must be accounted for when conducting socket qualification testing.

Conclusions

Thermo-electric modeling and experiments in this chapter demonstrated that Joule heating of stamped metal contacts can cause a significant temperature rise in LGA sockets. Stress relaxation work from chapter 3 concluded that the properties of the polymer housing were sensitive to temperature effects, and to greatly influence socket stress relaxation behavior. Higher socket temperatures driven by Joule heating were found to cause a greater reduction in the normal force, potentially leading to premature failure.

The factors that influence socket temperature rise and potentially contribute to earlier failure were examined in this study by using numerical modeling. A parametric study found that socket temperature rise was significantly influenced by processor temperature, contact pitch and the contact alloy properties, with contact alloy properties and processor temperature having the most significant effects. FEA results in this study therefore demonstrated that efficient thermal management that reduces processor temperatures and contact alloys with better thermo-electric

properties can mitigate Joule heating effects.

As the electronics industry moves towards finer interconnect, smaller pitch, higher processor temperatures and greater current densities, Joule heating will pose a greater reliability risk to high-density socket applications. Therefore quantifying socket temperatures that can occur in operation under electrical loading will be needed. This study indicates the need for conducting non-powered LGA socket qualification testing at temperatures that are higher than nominal processor temperatures in order to account for Joule heating of socket contacts and to assess the risk of failures relating to changes in mechanical properties. While a specific socket design was evaluated in this study and other socket designs may experience a different magnitude of Joule heating, the methodology outlined in this study can be used to quantify Joule heating effects. The resulting temperature estimates may be used by OEMs and socket manufacturers in order to test for and mitigate temperature-related failure mechanisms.

Chapter 5: A Methodology for Assessment of Life Expectancy in Stamped Metal Land Grid Array Sockets

Introduction

Joule heating work in chapter 4 and stress relaxation testing in chapter 3 concluded that temperatures driven by Joule heating can adversely affect the properties of the socket polymer housing thereby leading to premature failure. In this chapter a methodology to assess socket life expectancy under temperatures resulting from electrical loading was developed. Finite element modeling was used to determine socket time to failure. The visco-elastic behavior of the polymer housing was characterized, and the measured properties used to model stress relaxation in the socket being investigated, under temperature loads resulting from Joule heating. Lateral stress relaxation was observed, and the FEA was able to physically explain the mechanisms of socket stress relaxation when the polymer housing is not engaged.

Modeling Material Properties

The contact alloy was modeled as elastic while the polymer housing was modeled using visco-elastic properties. Visco-elastic behavior is evident from the stress relaxation testing as well as the force-strain behavior in chapter 3. Several researchers have also pointed out that liquid crystal polymers exhibit distinct viscoelasticity [44][45][46].

Even after accounting for Joule heating, operating temperatures in the contact

alloy (upto 150 °C) are still low enough that diffusion based creep mechanisms can be neglected. Diffusion based creep mechanisms are manifested at temperatures greater than 0.4 Tm (266 °C based on a melting temperature of 1075 °C for cu-be alloy) [54]. Dislocation based creep mechanisms which come into play at low temperatures and high stress can be ignored because of the multi-phase structure of the cu-be alloy. Several studies have reported good stress relaxation properties of C17200 copper beryllium alloy (80-90% remaining stress) for long term time intervals such as 10,000 hours at temperatures around 150 °C. The use of elastic properties for the contact alloy is therefore justified.

Determining Polymer Visco-Elastic Constants

Visco-elasticity and Generalized Maxwell Models

Polymers are generally described as visco-elastic because they exhibit the properties of both an elastic solid and a viscous fluid, depending on the temperature and the time scale involved. An elastic solid exhibits a definite shape, which deforms in response to an applied stress. Once the stress is removed the original shape is restored. Viscous fluids in contrast have no definite shape and flow irreversibly when an external force is applied [71].

Spring and dashpot models are generally used to describe polymer visco-elasticity. The spring represents an elastic solid where stress is proportional to strain, and the proportionality constant is the elastic or Young's modulus E.

$$\frac{\sigma}{E} = \varepsilon \qquad (5)$$

The dashpot represents a viscous fluid where the applied stress is proportional to the

strain rate. The proportionality constant is called the viscosity η.

$$\frac{\sigma}{\eta} = \dot{\varepsilon} \tag{6}$$

One of the simplest visco-elastic models is a Maxwell model which describes the behavior of a spring with modulus E and dashpot with viscosity η in series.

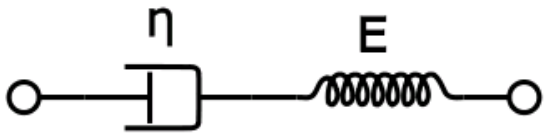

Figure 21: Maxwell element consisting of a spring and dashpot in series

The total strain ε in a Maxwell element in response to an applied stress is the sum of the individual strains in the spring and dashpot. Differentiating with respect to time in a stress relaxation test (constant strain) leads to

$$\dot{\varepsilon} = 0 = \dot{\varepsilon}_1 + \dot{\varepsilon}_2$$

$$\frac{\sigma}{E} = \varepsilon_1, \frac{\sigma}{\eta} = \dot{\varepsilon}_2$$

$$\frac{d\sigma}{dt}\frac{1}{E} + \frac{\sigma}{\eta} = 0 \tag{7}$$

where ε is the total strain, ε_1 is the strain in spring and ε_2 is the strain in dashpot. The constitutive relation for a single Maxwell element obtained by solving the above differential equation (equation 7) may be expressed as

$$\sigma = \sigma_0 e^{-Et/\eta}$$

where τ = η/E is called the retardation time. The above expression may be rewritten

in terms of moduli as

$$E(t) = E_o e^{-\frac{t}{\tau}} \tag{8}$$

with $E(t) = \frac{\sigma(t)}{\varepsilon}$

While equation 8 describes the constitutive relation for a single Maxwell element, real polymers however are typically described by using generalized Maxwell models which consist of a number of Maxwell elements in parallel (Figure 21). These models account for the fact that relaxation does not occur at a single time but as a distribution of times. The spring in parallel accounts for the fact that stress relaxation at infinite time is not zero. This behavior is represented by a Prony Series, where each Prony pair consists of two constants E_i and τ_i.

$$E(t) = E_e + \sum_{i=1}^{n} E_i e^{-\frac{t}{\tau_i}} \tag{9}$$

For details on polymer viso-elasticity the reader is urged to consult textbooks [71][55][72].

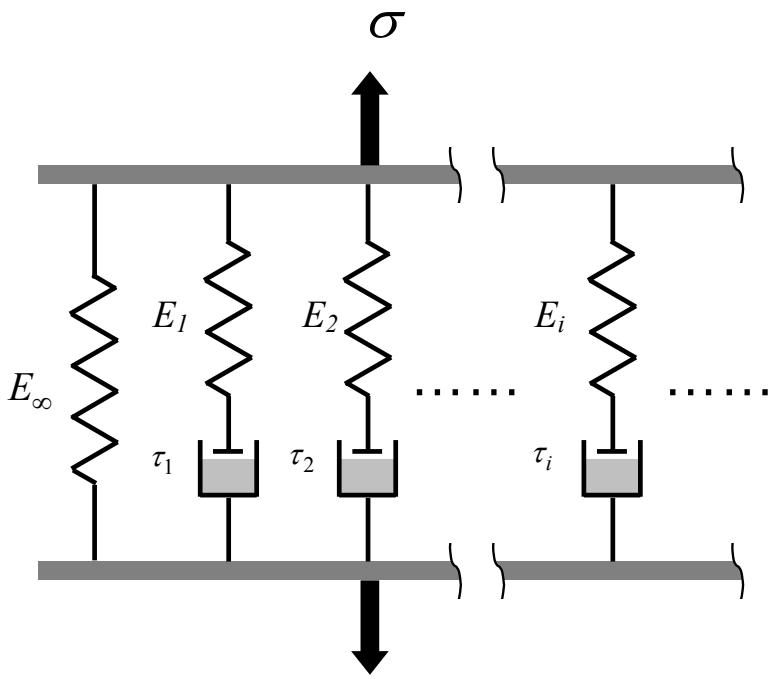

Figure 22: Generalized Maxwell Model

The Generalized Maxwell model does not take into account temperature effects. A time-temperature superposition approach which is based on a time-temperature equivalence will need to be used to account for temperature effects [71][55]. The time-temperature equivalence for polymers implies that testing at higher temperatures for a short period of time is equivalent to testing at lower temperatures for a longer time period. Based on time-temperature equivalence, stress relaxation test data can be used to construct a single master curve at a reference temperature. The individual curves are shifted in time horizontally until all the curves become superimposed, with the reference temperature curve remaining stationary. The shift factor which is the amount (a multiplication factor) that each curve is shifted with respect to the reference temperature is then plotted as a function of temperature.

The William-Landau-Ferry (WLF) shift is a commonly used time-temperature

superposition approach for polymers and is described by equation 10.

$$\log a_T = -\frac{C_1(T - T_{ref})}{C_2 + (T - T_{ref})} \tag{10}$$

where a_T is the shift factor at a given temperature T, T_{ref} is the reference temperature and C1 and C2 are material dependant constants.

Obtaining Visco-elastic and Temperature Constants for Socket Polymer Housing

Stress relaxation curves were obtained for the polymer housing at temperatures of 70, 90, 110 and 130 °C (Figure 23). Pieces of the socket housing with dimensions of 4 mm X 4 mm were cut out and the contacts removed. A sample size of 3 was used for each test condition.

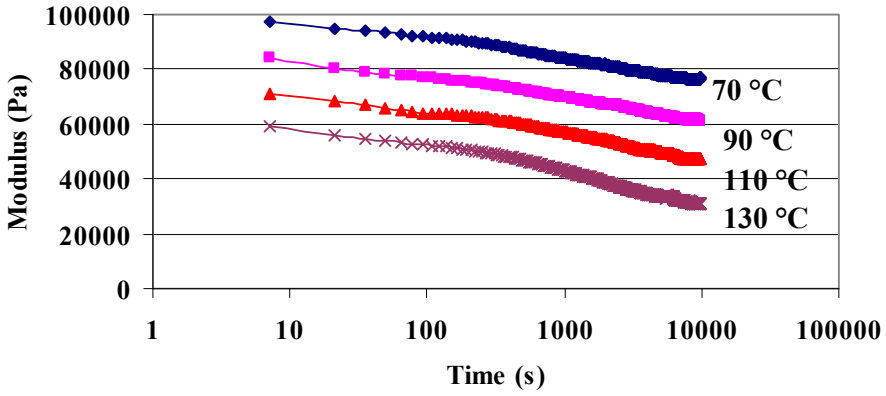

Figure 23: Stress Relaxation curves at 1% strain for polymer housing

The curves were then combined to yield a single master curve at 70 °C, by shifting the higher temperature curves in time to the right, until each curve overlapped with the lower temperature curve (Figure 24).

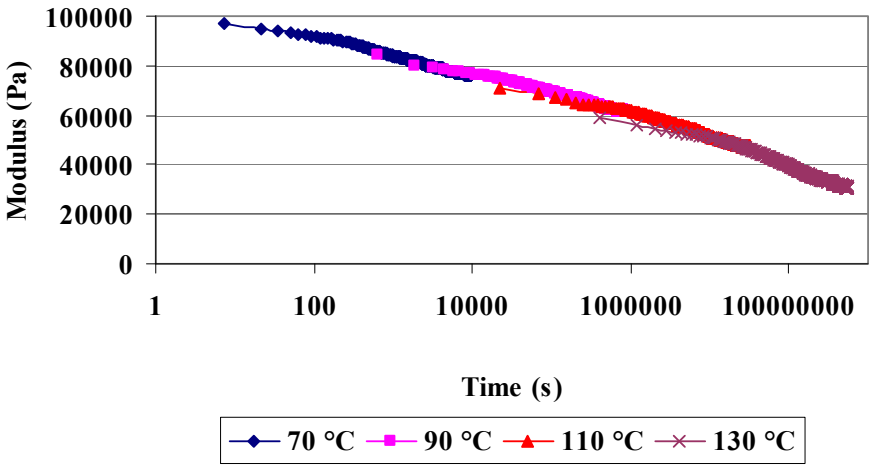

Figure 24: Master Curve at 70 °C for polymer housing

The shift factors aT were then curve fit to the WLF equation (equation 10) using Matlab, to determine the WLF constants C1 and C2. C1 and C2 were determined to be -10 and 150 respectively.

The master curve at 70 °C (Figure 24) was curve fit to the Prony series expression of equation 9 with 5 Prony pairs, using the curve fitting tool in ANSYS. Physically each Prony pair represents a relaxation mechanism or degree of freedom. Polymers undergo various relaxation mechanisms such as sliding of main chains, movement, wiggling, rotation and bond stretch of side chain functional groups. It is common in literature to use around 10 pairs in order to represent the different relaxation mechanisms in polymers ([46][49][83]). 5 Prony pairs were sufficient to model the relaxation mechanisms in this study. Curve fits were obtained using 4 (R2 =0.9) and 5 Prony pairs. 5 Prony pairs were found to be optimum (R2=0.99). The curve fit is illustrated in Figure 25 and Figure 26, using 4 and 5 Prony pairs respectively. The Prony pairs are reported in Table 7. Visco-elastic properties of the

polymer housing can therefore be described by using the Prony constants in a generalized Maxwell model and WLF constants together.

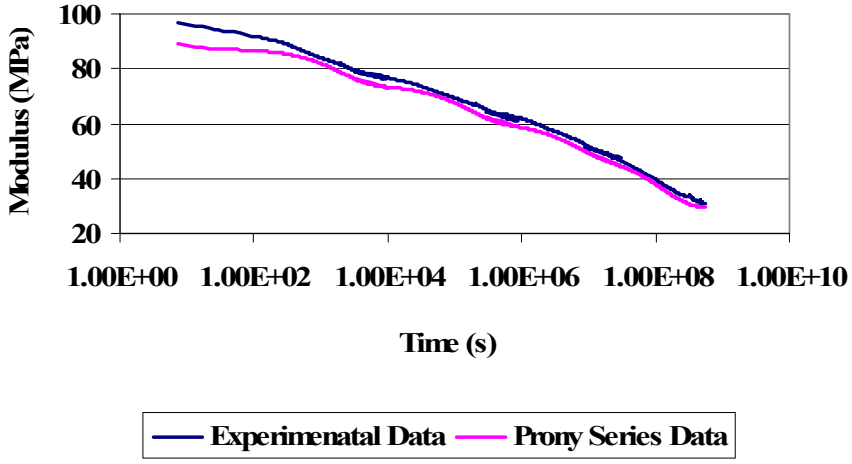

Figure 25: Master curve experimental vs. Prony series curve fit with 4 pairs (R2=0.9)

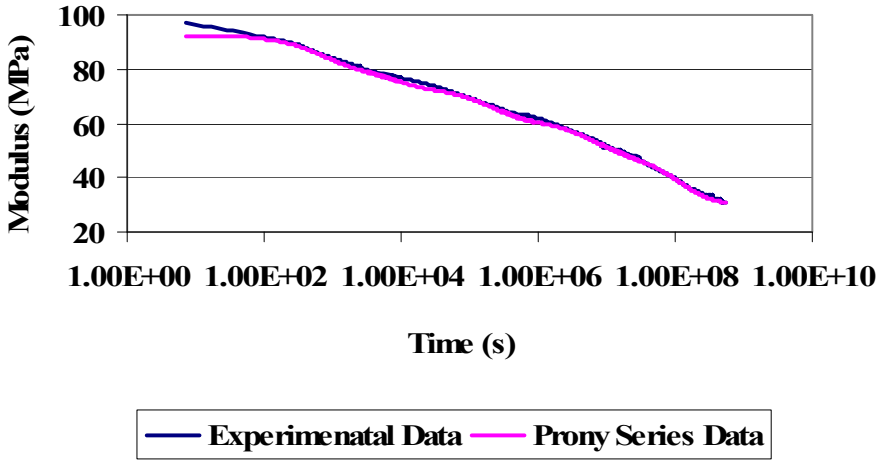

Figure 26: Master curve experimental vs. Prony series curve fit with 5 pairs (R2=0.99)

Input properties for the contact alloy included modulus values of 125 GPa, and Poisson's ratio of 0.3. The properties of stainless steel were used to model the

compression plates.

Table 7: Viscoelastic Prony pairs in Generalized Maxwell Model for polymer housing

Prony Pair	Ei	τ_i
1	0.11	710.61
2	0.09	6813
3	0.13	2.0845E+005
4	0.13	6.2385E+006
5	0.21	1.2429E+008

Finite Element Model

Finite element analysis was used to assess stress relaxation in the socket under temperature and displacement load conditions. To reduce the complexity and computational resources utilized, two dimensional, FE models that utilize the cross-sectional area are routinely used for the stress analysis. A single socket contact housed in the polymer housing was modeled to reduce model complexity.

. The various materials in the model (Figure 27) are distinguished based on their material properties. The figure also shows the FE mesh density utilized for the current study. Eight noded quadrilateral elements with quadratic displacement shape functions are used for the entire model. A 2-D plane stress analysis was conducted. The out-of-plane thickness of the various materials (contact alloy, polymer housing) are scaled to mimic their relative widths in the actual 3-D geometry of the socket.

In order to simulate the loading hardware used in an LGA socket assembly,

stainless steel blocks were used to compress the socket. Contact elements were used to simulate interface regions as opposed to permanently bonded structures. A displacement was applied on the top and bottom surfaces of the stainless steel blocks. Visco-elastic material properties were used to model the polymer housing, and elastic properties to model the contact alloy and loading blocks in the initial model. The revised model used a Ramberg-Osgood power law to model elasto-plastic properties for the contact alloy as will be discussed shortly.

Quadrilateral elements with mid-sided nodes were used and the model comprised of 2348 elements and 6909 nodes. A mesh optimization study was conducted and going to a finer mesh lead to a only a 1% change in the equivalent stress while increasing the number of elements by 30%. The coarser mesh was selected in order to reduce model complexity without significantly sacrificing accuracy.

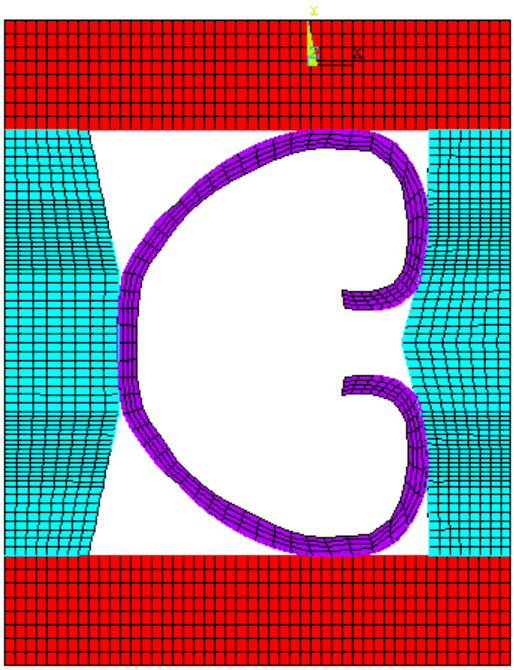

Figure 27: Mesh density and material types; C shaped contact – copper beryllium alloy, side walls- polymer housing, top and bottom compressing blocks –stainless steel

Two load steps were used to model stress relaxation behavior of the socket. In the first step the socket was compressed by applying a displacement load, which was ramped up in this step (The initial unmated state before the first load step is illustrated in Figure 13. At the end of the end of the first load step the unit cell is compressed as illustrated in Figure 27). In the second step the displacement was held constant and the loss in force was recorded over time. A temperature was specified for each of the test conditions.

Results and Discussion

The initial model which used elastic properties for the contact alloy, and a

default unit thickness of the materials, resulted in contact alloy stresses exceeding the yield strength of the material. Figure 28 illustrates how an elastic model can over predict stress when compared with a plasticity model for a given strain. Plastic properties were included in the model with n = 0.06, K = 1.4 GPa, in a Ramberg Osgood power law as indicated in Figure 28**,** and thickness effects were incorporated to mimic the ratios of widths in the actual three dimensional geometry of the socket. The resulting maximum stress was lower than the contact alloy yield strength (Figure 29).

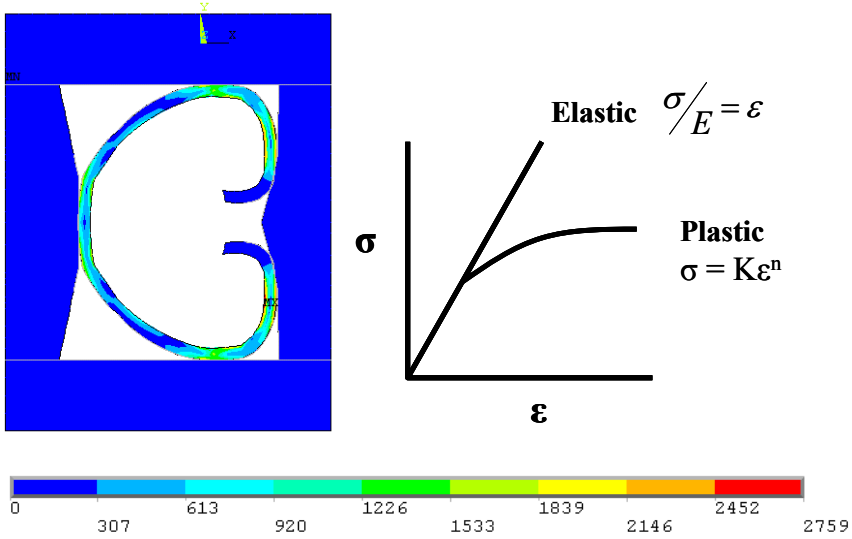

Figure 28: Equivalent stress distribution in MPa with elastic model for contact alloy. Maximum stress exceeds yield strength of contact alloy. The cartoon illustrates how an elastic model can overestimate the stress compared to a plasticity model at a given strain.

The revised model in Figure 29. shows a high stress concentration at regions where the polymer contacts the metal alloy. This constraint in the lateral direction can cause the polymer to stress relax laterally (x direction) over time. As a

consequence it takes less force to maintain a given deformation vertically (y direction), thereby leading to longitudinal stress relaxation.

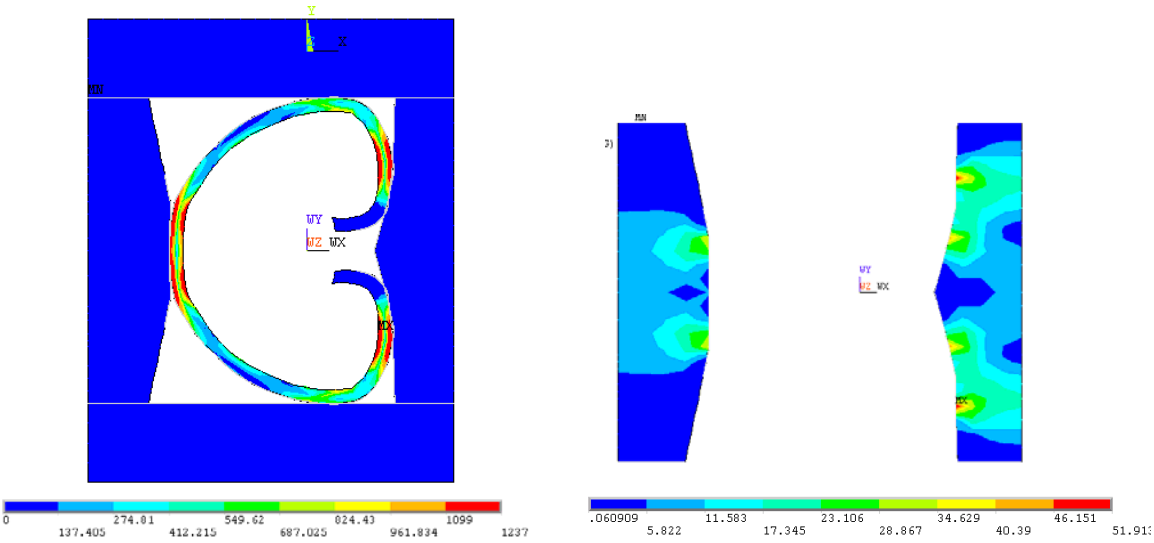

Figure 29: Stress distribution in socket in MPa under full compression. Note the high stress distribution in the polymer housing where the metal contacts the polymer

The stress relaxation data from the initial model showed extremely high values of force which were an order of magnitude greater than experimental data. After the model was revised by incorporating plasticity for the contact alloy as well as including thickness for the polymer and contact alloy, the model and experimental data showed reasonable agreement. The thickness values were changed from the default unit thickness for the 2D model to incorporate a contact/polymer thickness ratio of 0.3.

The revised model showed reasonable agreement between experimental and model data for a "strain" or normalized displacement of 15%. Sources of any discrepancy between experimental and model data include geometric approximations

in the finite element model and scatter in the experimental stress relaxation data (around 50 g as illustrated in appendix 3). The data is presented in Figure 30.

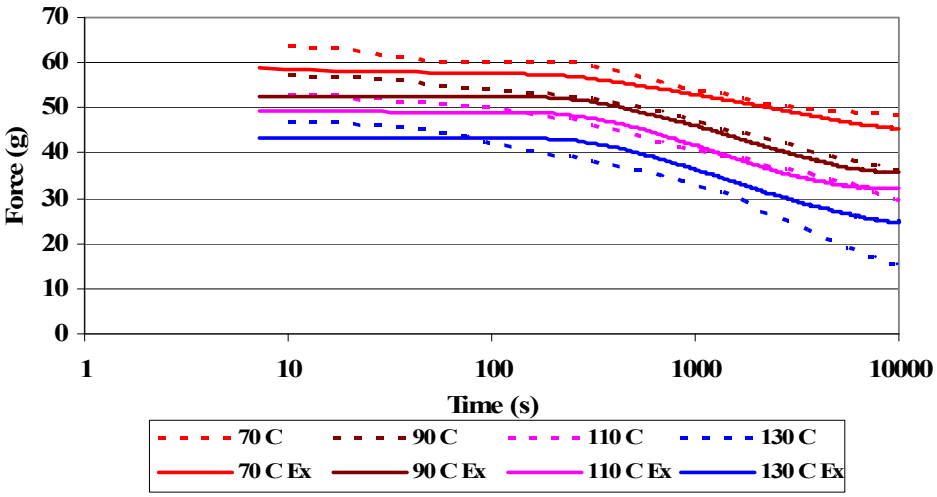

Figure 30: Model vs. Experimental Stress Relaxation curves at 15% strain. Dotted lines represent model while solid lines indicate experimental data.

A closer look at the data revealed a lag in all experimental stress relaxation data with an initial plateau region (Figure 31). This time delay may be reflective of the resistance the polymer chains face before they start to move and relieve the stress in response to an applied load. The resistance reflects the time taken to untangle, slide, move and overcome friction.

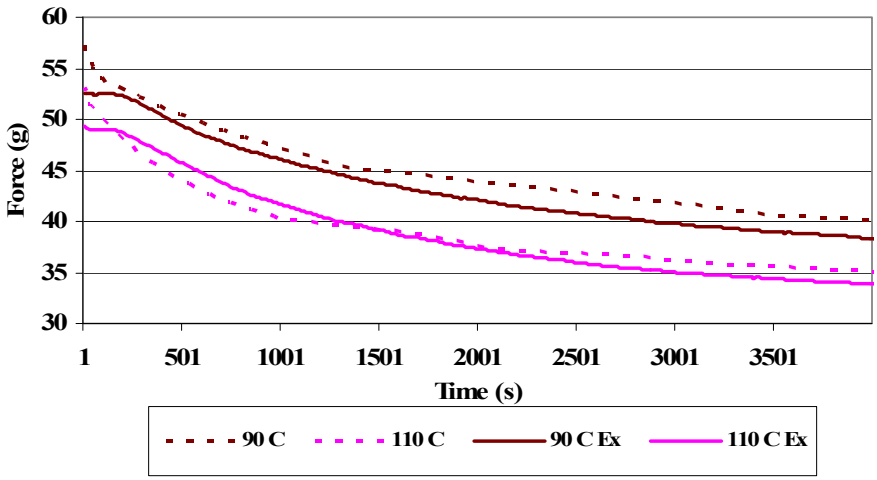

Figure 31: Initial Lag in Experimental Relaxation data

Lateral stress relaxation was observed in the FEA model as indicated in Figure 32. The polymer is under constraint in the lateral direction as demonstrated in Figure 28. Over time the polymer relaxes laterally, thereby contributing to stress relaxation in the longitudinal direction by requiring less force to maintain a given deformation over time. Earlier work in chapter 3 reported that stress relaxation was observed experimentally when the compressive force was low enough that the C-shaped contacts carried the entire load, without the polymer being engaged. The FEA model was able to explain longitudinal stress relaxation as being a consequence of lateral polymer relaxation. The FEA therefore provides an understanding of the physical mechanisms of stress relaxation in LGA sockets while under contact loading.

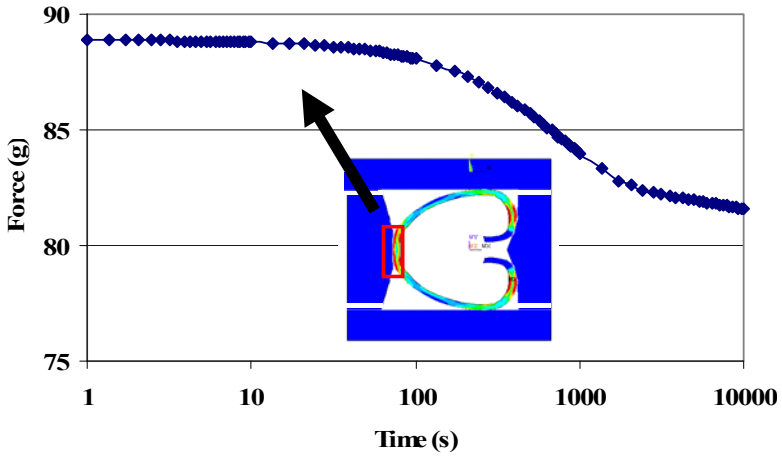

Figure 32.: Stress Relaxation curves in the lateral direction (Fx) at 70 °C, 15% strain, polymer not engaged

Effect of Joule Heating on Stress Relaxation Using Finite Element Analysis

Previous work in chapter 4 was able to determine average polymer and contact alloy temperatures as a function of current through the socket contacts using finite element analysis. The average temperatures obtained from the thermo-electric FEA were used as an input to the stress relaxation FE model, in order to determine stress relaxation time to failure for upper and lower bounds of processor temperature and current per contact for power contacts.

The failure criterion for resistance in order to determine time to failure was based on the EIA specification for LGA sockets. The force-resistance behavior of Figure 9, indicates that the stable contact resistance is centered around 10 mΩ. As per the EIA specification for LGA sockets, an increase in contact resistance by 20 mΩ or more is considered a failure. The minimum force, based on Figure 9, to satisfy the failure criterion is therefore 18g. Figure 33 is a representative stress relaxation curve from the FEA model that demonstrates how the time to failure was determined. The

dot indicates the time when a force of 18 g was reached.

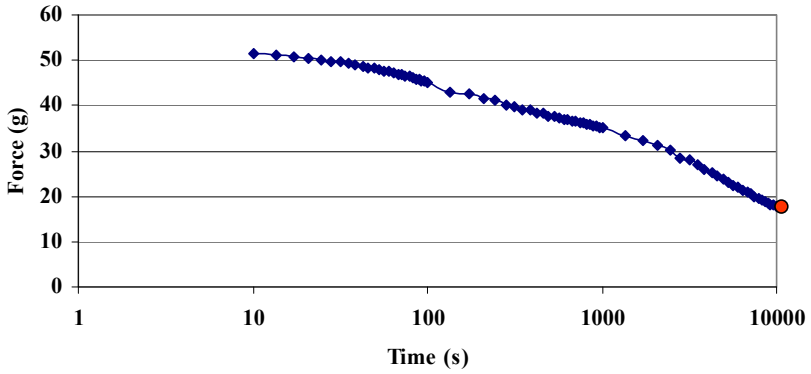

Figure 33: Stress Relaxation curves at 100 °C processor temperature, 3 A current and 15% strain

The times to failure were obtained for upper and lower bounds of processor temperature and current per pin for power contacts. The time to failure was also calculated according to the EIA high temperature life specification which recommends conditions of 85 °C for 500 hours. Based on the results of Table 8, the EIA specification represents benign conditions when compared with all but one other condition. Qualification testing should account for the most severe conditions possible, in order to rule out field failures.

Table 8: Time to failure prediction from FEA model for 15% strain using 18 g as the minimum force criterion

Current (A)	Processor Temp. (°C)	Time to Failure (hrs) per contact
3	100	2.8
3	70	55
1	100	58
1	70	1378
0 (EIA)	85	168

Stamped metal sockets in the field are able to pass the EIA specification test at 85 °C for at least 1000 hours. The stress relaxation model in this study however predicts a time to failure that is approximately five times lower. A sensitivity analysis for the stress relaxation model was conducted using 14 g as failure criterion, instead of the original 18 g. The time to failure approximately doubled when a lower value of force (14 instead of 18 g) was used as the failure criterion (Table 9, Table 10, and Table 11). The data therefore shows that time to failure is sensitive to the force used as the failure criterion.

Table 9: Time to failure prediction from FEA model for 15% strain using 14 g as the minimum force criterion

Current (A)	Processor Temp. (°C)	Time to Failure (hrs) per contact
3	100	5
3	70	99
1	100	108
1	70	2478
0 (EIA)	85	378

Stress relaxation time to failure data was also obtained for 12 and 18% "strain" in an effort to capture a distribution of time to failure. The data is presented in Table 10 and Table 11.

Table 10: Stress relaxation time to failure at 18% "strain" with 18 g and 14 g as the failure criterion

Current (A)	Processor Temp. (°C)	Time to Failure (hrs) per contact (18 g/14 g)
3	100	4.8/8.8
3	70	80/162
1	100	88/168
1	70	1978/3778
0 (EIA)	85	268/570

Table 11: Stress relaxation time to failure at 12% "strain" with 18 g and 14 g as the failure criterion

Current (A)	Processor Temp. (°C)	Time to Failure (hrs) per contact (18 g/14 g)
3	100	2/3.8
3	70	28/57
1	100	33/58
1	70	978/1578
0 (EIA)	85	127/206

Stress relaxation time to failure was also obtained from the model using 10 g as the failure criterion, at the EIA specified condition of 85 °C (Table 12). At 18% "strain" the time to failure is 1000 hours, which is in the ballpark of manufacturer test data. Therefore the time to failure is sensitive to the minimum force used as the failure criterion, which in turn depends on the contact finish. Further the contact load also plays a role. The 18% strain condition represents maximum compression and therefore the highest force before the polymer becomes engaged. This condition may be most representative of operational LGA socket loading where manufacturers recommend the use of the highest possible load without engaging the polymer housing.

Table 12: Stress relaxation time to failure at EIA condition based on 10g as the minimum force

Strain (18%)	Processor Temp. (°C)	Time to Failure (hrs) per contact(10g)
18	85	1000
15	85	678
12	85	478

Some possible reasons for the discrepancy wherein the model used in this study over predicts time to failure include the following:

1. Soft gold is used on the microprocessor pads in an LGA assembly, which may result in a lower contact resistance for a given force (due to lower hardness

and resistivity). Hard golds have about twice the hardness and can have resistivities three times or more when compared to soft gold. The knee of the curve may be to the left of the behavior represented in this study.

2. The full assembly stickup was not considered in this study. There may be effects from the assembly that limit stress relaxation, and this needs further evaluation.

Summary and Conclusions

A methodology to assess socket life expectancy under time, temperature and deformation loads was developed in this chapter. This study examined the influence of Joule heating on socket stress relaxation behavior using numerical modeling. The polymer housing was found to exhibit distinct visco-elastic behavior and its properties were found to be sensitive to temperature. A generalized Maxwell model was determined to fit the polymer stress relaxation data well and a time-temperature superposition approach was used to model temperature effects. The measured visco-elastic properties were used to model the polymer material properties in a finite element model of the socket. Elasto-plastic behavior was modeled for the contact alloy.

The resulting FEA was able to confirm relaxation in the lateral direction. This explained the phenomenon of relaxation vertically even when there was no polymer engagement in the Z direction. Further there was good agreement between the stress relaxation model and experimental data. A time to failure prediction was then made based on the model for upper and lower bounds of processor temperature and current

per pin for the power contacts. The results indicated that the EIA specification for high temperature life test in LGA sockets represents one of the most benign set of conditions. Socket test conditions need to account for higher temperatures resulting from Joule heating of the socket contacts.

Chapter 6: Contributions, Recommendations and Future Work

Summary

This study demonstrated that Joule heating of stamped metal contacts is an important design consideration that can impact the reliability of stamped metal land grid array sockets. The resulting higher temperatures were found to adversely affect the mechanical properties of the socket housing and cause premature socket failure.

A methodology to determine socket temperatures under electrical loading was provided. An understanding of operating temperature environments will allow socket manufacturers and OEMs to test for and mitigate failure mechanisms under thermal aging. The factors that influence socket temperatures under electrical loading were examined. Contact alloy, processor temperature and contact pitch were all found to significantly influence socket temperatures, with the contact alloy and processor temperature having the most significant effects.

Further a methodology to determine socket life expectancy under temperature and deformation loads was developed. Visco-elastic behavior of the polymer housing was confirmed, and experiments were conducted to determine visco-elastic properties of the socket polymer housing. The measured properties were used to model the stress relaxation behavior of the socket. The mechanism of socket stress relaxation was explained as being due to lateral stress relaxation in the polymer housing. Numerical modeling determined that higher temperatures due to Joule heating decreased stress relaxation time to failure.

Contributions from this Study

- This study identified Joule heating as a necessary consideration in stamped metal socket design. A methodology to determine socket temperatures under electrical loading, which will enable testing and mitigation of failures under high temperature environments, was provided.
- This study also provided a methodology for assessing life expectancy of stamped metal land grid array sockets. Results from this study concluded that socket temperatures due to Joule heating can significantly exceed temperatures recommended in standards based testing, indicating the need for socket testing with power or at temperatures that are reflective of Joule heating.
- This study identified polymer relaxation as a principle contributor to failure in stamped metal LGA sockets under high temperature environments
    - Polymer visco-elastic properties over use and test conditions were determined.

Future Work

The current study investigated the effect of DC current, while real world scenarios use AC current for signal applications. As signal frequencies increase, the signal will concentrate in the skin of the conductor. Any degradation would manifest itself as noise, and show an increased sensitivity to contact issues. While currents are typically low in signal applications, the signal concentration in the skin would increase the bulk resistance significantly, making Joule heating a reliability concern

as signal frequencies increase. Investigation of Joule heating under AC current is suggested as a future area of study.

A further suggestion for future study to investigate the thermal and structural behavior of a full socket in order to examine contact to contact variations, and their effect on socket reliability. Further assembly effects which were not evaluated in this study, and that consider all the individual layers of the stickup, is suggested for future study.

Recommendation for Revision of LGA Socket Specifications

The electronics industry alliance (EIA) specification for LGA sockets [52] calls for sequential testing by dividing a socket population into different groups with each going through a series of tests such as vibration, thermal cycling and high temperature life. The high temperature life test conditions are specified as 85 °C for 500 hours without power as part of the sequential testing. Processors with chip operating temperatures greater than 100 °C are currently in use [79], while the socket specification calls for less stringent conditions of 85 °C for high temperature life testing.

The current EIA specification does not reflect the usage conditions of current day microprocessors or the additional temperature rise due to the passage of current through the socket contacts. The LGA socket specification needs to be revised to account for higher processor temperatures as performance requirements increase, the more severe temperature environments for socket contacts with current, and also be tied to socket life expectancy. By testing for worst case conditions that can arise

during operation failures in the field can be mitigated.

Appendix 1: Polymer Melting Temperature

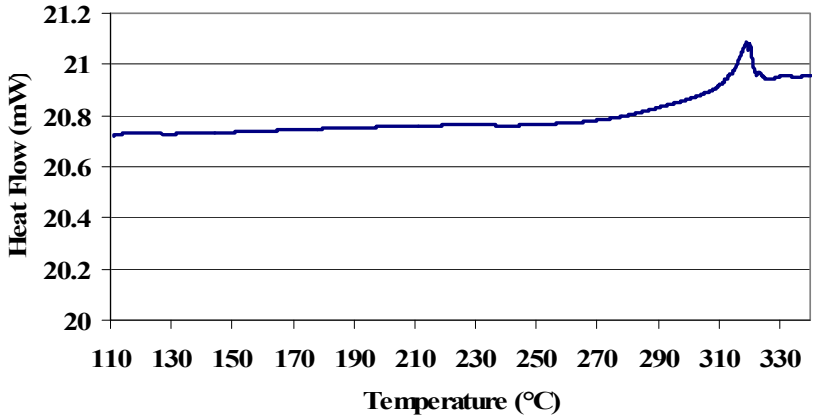

Figure 34: DSC curve of polymer showing melting transition at 320 °C

Appendix 2: Determining Thermal Contact Conductance

Heat transfer across a contact interface occurs by conduction through both the solid contact spots or A-spots as well as through the gas gaps.

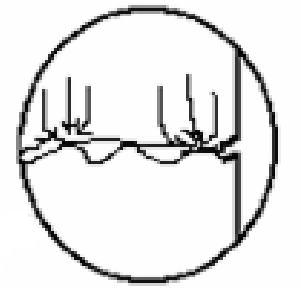

Figure 35: Illustration of a contact interface with A-spots or asperities

The overall contact conductance is the sum of the solid and gas contact conductances.

$$h = h_s + h_g$$

where h is the total contact conductance, h_s is the solid contact conductance and h_g is the gas contact conductance. h_s and h_g may be estimated using the equations 11 and 12.

$$h_s = 1.13K \frac{\tan\theta}{\sigma}\left(\frac{p}{H}\right)^{0.94} \qquad (11)$$

where p is the nominal contact pressure, H is the hardness of the contact finish, K is the mean thermal conductivity of the interface, tan θ is the mean absolute asperity slope and σ is the RMS roughness .

$$h_g = \frac{K_g}{\delta + 2g} \qquad (12)$$

where K_g is the thermal conductivity of the gas, δ is the mean physical gap and g is the temperature jump distance. For more details and for alternate equations on

thermal conductance the reader is urged to consult references in the literature [62][63][84].

Appendix 3: Scatter in Stress Relaxation Curves

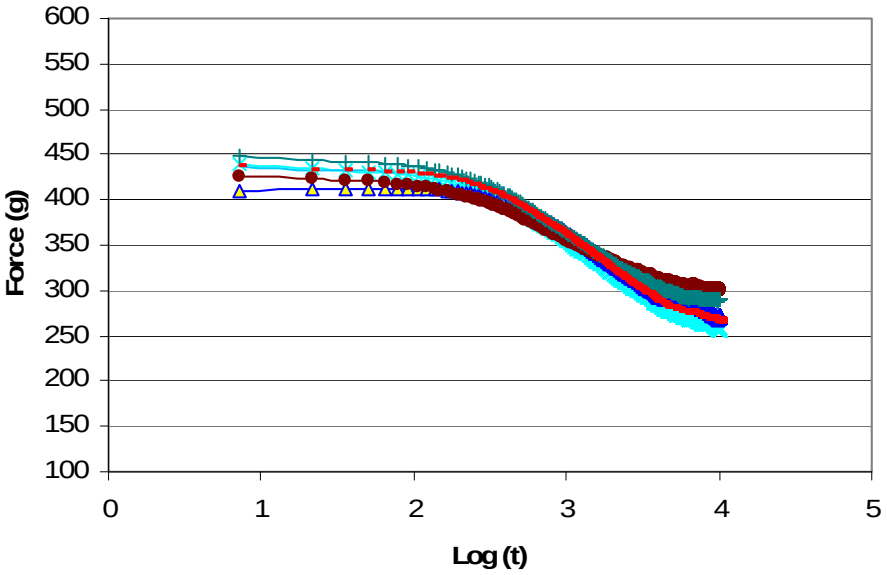

Figure 36: Representation of scatter in stress relaxation curves

Bibliography

[1] International Technology Roadmap for Semiconductors (ITRS), 2007, 2008 update, www.itrs.net, Last accessed May 24th, 2010.

[2] Pope, R. A.; Schoenbauer, D.J., "Temperature rise and its importance to connector users" in 1987 Proceedings of the 37th Electronic Components Conference 1987. pp. 24-31, xii+651, New York, NY, USA, Boston, MA, USA, IEEE, Conference Paper.

[3] Liu, W. , Pecht, M., Martens, R., " IC Component Sockets: Applications and Challenges", International Microelectronics And Packaging Society,Vol.24, Issue 1, pp. 61-67, 2001

[4] Liu and M. Pecht, " IC Component Sockets", Wiley Interscience, John Wiley and Sons Inc., Hoboken, NJ. 2004 W.

[5] Karl Puttlitz and Paul A. Totta, *Area Array Interconnection Handbook*, New York, Kluwer Academic Publishers, 2001, pp. 432-434.

[6] Corbin, J. S, Ramirez, C. N, Massey, D., Land grid array sockets for server applications, IBM Journal of Research and Development, Nov 2002, Volume 46, Issue 6, pp. 763-778.

[7] Liu, W. and Pecht, M., "Fundamental Reliability Issues Associated with a Commercial Particle-in-Elastomer Interconnection System", IEEE Transactions on Components and Packaging Technologies, Sep. 2001, Vol. 24, No. 3, pp. 520-525.

[8] Roland Timsit, Book Chapter, Electrical Contact Resistance: Fundamental

Principles in Electrical *Contacts: Principles and Applications*, Edited by Paul Slade, New York : Marcel Dekker, 1999.

[9] M. Antler, "Gold plated contacts: effect of thermal aging on contact resistance", Proceedings of the Forty-Third IEEE Holm Conference on Electrical Contacts, 1997., , 20-22 Oct 1997, page(s): 121 – 131, Philadelphia, PA.

[10] Haque, C.A., "Characterization of metal-in-elastomer connector contact material", Proceedings of the Thirty Fifth Meeting of the IEEE Holm Conference on Electrical Contacts, 1989., September 18-20 1989, pp: 117-121,Chicago, IL, USA

[11] Rosen, G. Robinson, P.T. Florescu, V. Singer, M.T., "A comparison of metal-in-elastomer connectors-the influence of structure on mechanical and electrical performance", Proceedings of the Thirty-Sixth IEEE Holm Conference on Electrical Contacts, 1990., and the Fifteenth International Conference on Electrical Contacts , Aug 1990, pp: 151-165, Montreal, Que., Canada.

[12] Fulton, J.A. Horton, D.R. Moore, R.C. Lambert, W.C. Jin, S. Opila, R.L. Sherwood, R.C. Tiefel, T.H. Mottine, J.J., "Electrical and mechanical properties of a metal-filled polymer composite for interconnection and testing applications", 39th Electronic Components Conference, 1989. Proceedings., 22-24 May 1989, pp: 71-77, Houston, TX, USA

[13] Brodsky, W.L. , Knight, A.D. Macek, T., "Featured elastomer design for connector applications", 43rd Electronic Components and Technology

Conference, 1993. Proceedings., June 1-4 1993, pp: 465-467, Orlando, FL, USA

[14] Weifeng. Liu, Michael. Pecht and Jingsong Xie, Fundamental Reliability Issues Associated with A Commercial Particle-in-Elastomer Interconnection System, IEEE Transactions on Components and Packaging Technologies, Volume 24, No. 3, pp. 520-525, September, 2001.

[15] Weifeng Liu, Mikyoung Lee, Michael Pecht and Rod Martens, "An Investigation of the Contact Resistance of a Commercial Elastomer Interconnect Under Thermal and Mechanical Stresses," *IEEE Transactions on Device and Materials Reliability*, Vol.3, No.2, June 2003, pp. 39-43

[16] S. Yang, J. Wu, and M. Pecht, "Electrochemical Migration of Land Grid Array Sockets under Highly Accelerated Stress Conditions," in Proc. 51st IEEE HOLM Conference on Electrical Contacts, Chicago, IL., Sep. 26-28, 2005, pp. 238-244

[17] Shuang Yang, Ji Wu and Michael G. Pecht , "Reliability Assessment of Land Grid Array Sockets Subjected to Mixed Flowing Gas Environment" , IEEE Transactions on Reliability, Vol. 58, No. 4, pp. 634-640, December 2009

[18] Yang, S., Wu, J., Tsai, D., and Pecht, M., "Contact Resistance Estimation for Time-Dependent Silicone Elastomer Matrix of Land Grid Array Socket", IEEE Transactions on Components and Packaging Technologies, March 2007, Vol. 30, No. 1, pp. 81-85.

[19] Jingsong Xie, Michael Pecht, David DeDonato, and Ali Hassanzadeh "An Investigation on Mechanical Behavior of Conductive Elastomer

Interconnects," Microelectronics Reliability, vol. 41, no. 2, pp. 281-286, Dec. 2001.

[20] Leoncio L. Lopez, Vidyu Challa, and Michael Pecht, "Assessing the Reliability of Elastomer Sockets in Temperature Environments", *IEEE Transactions on Device and Materials Reliability*, Vol. 9, Issue 1, pp. 80-86, March 2009

[21] L.D. Lopez and M.G. Pecht, Modeling of IC Socket Contact Resistance for Reliability and Health Monitoring Applications, *IEEE Transactions on Reliability,* Vol. 58, No. 2, pp. 264-270, June 2009.

[22] Guarin, F.J. Katsetos, A.A., " Solderless high-density interconnects for burn-in applications", 42nd Electronic Components and Technology Conference, 1992. Proceedings., May 1992 page(s):263-267 San Diego, CA, USA

[23] Yang, Shuang, Wu, Ji, and Pecht, Michael " Reliability assessment of High Density IC Sockets and Tests for the Causes of Failure", CALCE consortium report 2004.

[24] Almquist, F. " Button Contacts for Liquid Nitrogen Applications 39th Electronic Components Conference, 1989. Proceedings., May 1989, pp: 88-91, Houston, TX.

[25] Robert R. Marker, "Button Board Contacts, A solution for High Speed Signal Matched Impedance Interconnect", Connection Technology, February 1992, pages 28-31.

[26] Harris, D.B., and Pecht, M. "A Reliability Study of Fuzz Button Interconnects", Circuit World , 1995, Vol. 21, No. 2, pp. 12-18.

[27] Electrical Contacts: Principles and Applications, Edited by Paul Slade, New York : Marcel Dekker, 1999

[28] David W. Song, Ashish Gupta, and Chia-Pin Chiu, "Thermal Analysis of Microprocessor Sockets", The Tenth Intersociety Conference on Thermal and Thermomechanical Phenomena in Electronics Systems, 2006. ITHERM '06, May 30 2006-June 2 2006, San Diego, CA, 126 – 131

[29] Ahmad, M.; Sitaraman, S.K.; "Study of coupled thermal electric behavior of compliant micro-spring interconnects for next generation probing applications" IEEE Transactions on Components and Packaging Technologies, Volume: 26 , Issue: 2

[30] McGowan, D.; "Power connector evaluation for thermal performance", Applied Power Electronics Conference and Exposition, 2008. APEC 2008. Twenty-Third Annual IEEE, 2008 , Page(s): 1597 – 1601

[31] Wang Xin, Xu Liang-jun, "Finite element model analysis of thermal failure in connector", Journal of Zhejiang University - Science A, Issue Volume 8, Number 3 / March, 2007, Pages 397-402.

[32] Dunn, B. D. , "Mechanical and electrical characteristics of tin whiskers with special reference to spacecraft systems", ESA Journal , vol. 11, no. 4/vol. 12, no. 1, 1987/1988, pages 1-17.

[33] James H. Richardson, and Brian R. Lasley, "Tin Whisker Initiated Vacuum Metal Arcing in Spacecraft Electronics," 1992 Government Microcircuit Applications Conference, Vol. XVIII, pages 119 - 122, November 10 - 12, 1992.

[34] Runde, M.; Hodne, E.; Totdal, B.; "Current-induced aging of contact spots", Proceedings of the Thirty Fifth Meeting of the IEEE Holm Conference on Electrical Contacts, 1989 , Page(s): 213 – 220

[35] Frank Dunlevy, "Spring Loaded, An Old Alloy Meets New Component Needs", Components, Australian Electronics Engineering March 1996, pages 52-56.

[36] Tracy, N.L.; Rothenberger, R.; Copper, C.; Corman, N.; Biddle, G.; Matthews, A.; McCarthy, S, "Array sockets and connectors using MicroSpringTM technology", Electronics Manufacturing Technology Symposium, 2000. Twenty-Sixth IEEE/CPMT International, 2000 , Page(s): 129 – 140.

[37] cLGA® sockets: Qualification, Production, and Performance Ready, Neidich, D. In Twenty Seventh Annual IEEE/CPMT/SEMI International Electronics Manufacturing Technology Symposium (Cat. No.02CH37299), 2002, pp., pp. 105-9, iv+429 pp. Piscataway, NJ, USA; San Jose, CA, USA : IEEE, Conference Paper. (AN: 7492484),.

[38] Vidyu Challa, Leon Lopez, Michael Osterman and Michael Pecht, Stress Relaxation Testing in Stamped Metal Land Grid Array (LGA) Sockets, *IEEE Transactions on Device and Materials Reliability*, Vol.10, No.1, pp.55-61, March 2010.

[39] Cinch Iq, Datasheet, http://www.cinch.com/products/electronic-communication-systems/z-axis-compression/iq, Last accessed January 5, 2010.

[40] Tyco Mc-LGA socket, datasheet, http://www.tycoelectronics.com/catalog/Presentations/1773377_mc-lga.pdf, Last accessed January 5, 2010

[41] Fox, A. Fiuchs, E.O; "Mechanical Properties in Bending at Elevated Temperature of High Strength Copper Alloy Flat Spring Materials", Journal of Testing and Evaluation. Vol. 6, no. 3, pp. 211-220. May 1978

[42] E. Shapiro and J.A. Bloome, "A New High Strength Bronze for Contacts, Terminals and Connectors", Olin Corporation.

[43] Properties of Brush Wellman High Performance Strip Materials. http://www.brushwellman.com/WorkArea/showcontent.aspx?id=1750, Last accessed January 5, 2010

[44] Witold Brostow, "Mechanical and thermophysical properties of polymer liquid crystals", Chapman & Hall, 1998

[45] I. M. Ward J. Sweeney, "An Introduction to the Mechanical Properties of Solid Polymers" , Second Edition, Wiley 2004

[46] L. Gervat, M. R. Mackley, T. M. Nicholson, A. H. Windle, The Effect of Shear on Thermotropic Liquid Crystalline Polymers , Philosophical Transactions: Physical Sciences and Engineering, Vol. 350, No. 1692 (Jan. 16, 1995), pp. 1-27

[47] Elvira Somma, Rossana Iervolino1 and Maria Rossella Nobile, The viscoelasticity of thermotropic liquid crystalline polymers: effects of the chemical composition, Rheologica Acta, Issue Volume 45, Number 4 / April, 2006

[48] E. Shiva Kumar, C.K. Das, Mechanical, dynamic mechanical properties and thermal stability of fluorocarbon elastomer-liquid crystalline polymer blends, Polymer Composites, Volume 26 Issue 3, Pages 306 – 315, Feb 2005

[49] Chae, Seung-Hyun; Zhao, Jie-Hua; Edwards, Darvin R.; Ho, Paul S., "Characterization of the Viscoelasticity of Molding Compounds in the Time Domain" Journal of Electronic Materials , Volume 39, Number 4 / April, 2010

[50] E328-02 ASTM Standard Test Methods for Stress Relaxation Tests for Materials and Structures, Apr 2003, pp. 404-422.

[51] Kulwanoski, G., Gaynes, M., Smith, A., Darrow, B., "Electrical Contact Failure Mechanism Relevant to Electronic Packages", Electrical Contacts, Proceedings of the Thirty-Seventh IEEE Holm Conference, 1991, New York, NY, pp. 184-92.

[52] EIA 540B0AE, "Detailed Specification for Production Land Grid Array Socket (LGA) for Use in Electronic Equipment", June 2000.

[53] Lopez, L., and Pecht, M., "Assessing the Temperature and Relative Humidity Environment of IC Sockets in Enterprise Servers for Prognostics and Health Monitoring", International Conference on Prognostics and Health Management, 6-9 Oct. 2008, pp. 1-6.

[54] Dowling, N. "Mechanical Behavior of Materials", Third Edition, Pearson Prentice Hall, 2007.

[55] Engineered Materials Handbook Vol. 2: Engineering Plastics, ASM International, 1988

[56] Evaristo Riande, Ricardo Diaz-Calleja, Margarita G. Prolongo, Rosa M.,

"Polymer Viscoelasticity: Stress and Strain in Practice", CRC Press, 2000, New York, NY

[57] Ranganthan, M., and Pecht, M., "Development of an Automated Contact Resistance Probe" 27th Annual Connector and Interconnection Symposium and Trade Show, IICIT, Inc., Boston, MA. Sep. 19-21, 1994.

[58] Rod Martens and M. Pecht, "The Effect of Wipe on Corroded Nickel Contacts", Conference on Electrical Contacts. Joint with the 18th International Conference on Electrical Contacts, New York, NY, 1996, pp. 342-351.

[59] ANSYS 11, User Manual

[60] XANSYS ANSYS users forum, www.xansys.net

[61] A Heat Transfer Textbook, Third Edition, John H. Lienhard IV, John H. Lienhard V, Phlogiston Press; 3rd edition (August 5, 2003)

[62] C. V. Madhusudana, Thermal contact conductance, Springer 1996

[63] Yovanovich, M.M, Four decades of research on thermal contact, gap, and joint resistance in microelectronics, IEEE Transactions on Components and Packaging Technologies, , June 2005, Volume: 28 Issue:2, page(s): 182 – 206.

[64] www.matweb.com, C17200 material properties, last accessed July 27th, 2010

[65] Frank Dunlevey, "Connector Reliability: The Role of Contact Spring Alloys" http://www.connectorsupplier.com/tech_updates_Wellman_spring_alloys_3-6-07.htm, March 2007, Last accessed July 27th, 2010.

[66] Half normal probability plot, http://www.itl.nist.gov/div898/handbook/pri/section5/pri598.htm, Last

accessed July 27th, 2010

[67] C.F. Jeff Wu, Michael Hamada, "Experiments : planning, analysis, and parameter design optimization" New York : J. Wiley, 2000.

[68] R software, The R Project for Statical Computing, http://www.r-project.org/, Last accessed January 5, 2010.

[69] Properties of Brush Wellman High Performance Strip Materials. http://www.brushwellman.com/WorkArea/showcontent.aspx?id=1750, Last accessed January 5, 2010.

[70] Website, "Processor Electrical Specifications", http://mysite.verizon.net/pchardwarelinks/elec.htm, last accessed November 6, 2010.

[71] Roderic S. Lakes, "Viscoelastic Solids", CRC Press, Mechanical Engineering Series, 1998

[72] J. E. Soussou, F. Moavenzadeh, and M. H. Gradowczyk, "Application of Prony Series to Linear Viscoelasticity", Journal of Rheology, Volume 14, Issue 4, December 1970, pp.573-584

[73] Mroczkowski, R.S., "Electronic Connector Handbook" , McGraw-Hill, New York, 1998

[74] Hassenzadeh, A., Dedonato, D., Xie, J., Hillman, C., Sandborn, P., and Pecht, M., "Assessing the Operating Reliability of Land Grid Array Elastomer Sockets", IEEE Transactions on Components and Packaging Technologies, March 2000,Vol. 23, No. 1, pp. 171-176

[75] Harris, D.B., and Pecht, M. "A Reliability Study of Fuzz Button

Interconnects", Circuit World , 1995, Vol. 21, No. 2, pp. 12-18.

[76] Holm, R. "Electric Contacts", Springer-Verlag, Berlin, 1968.

[77] Lopez, Leon, and Pecht, Michael, "Assessing the Temperature and Relative Humidity Environment of IC Sockets in Enterprise Servers for Prognostics and Health Monitoring", International Conference on Prognostics and Health Management, 6-9 October 2008, Denver, Colorado, pages 1-6.

[78] Lopez, L. D. Nathan, S. Santos, S. "Preparation of Loading Information for Reliability Simulation" IEEE Transactions on Components and Packaging technology, Volume: 27, Issue: 4, pp. 732-735.

[79] Website, "Processor Electrical Specifications", http://users.erols.com/chare/elec.htm, last accessed May 6, 2009

[80] Cinch Iq Stamped Metal Socket Design Guide, http://www.cinch.com/images/brochures/1208182282-iQ_Design_Guide.pdf, last accessed May 6, 2009

[81] Website, "A Comparison of the cLGA® Testing to the Requirements of the EIA Specification", http://www.lgasockets.com/qual/comp.pdf, last accessed May 6, 2009

[82] J. Xie, et al., "Assessing the Operating Reliability of Land Grid Array Elastomer Sockets," IEEE Transactions on Components and Packaging Technologies, vol. 23, no. 1, pp. 171-176, Mar. 2000.

[83] Bongtai Han and Changsoo Jang, CALCE consortium report C08-17, Accelerated Testing Guideline of COF Package Assembly, December 2008.

[84] M. M. Yovanovich, J. R. Culham and P. Teertstra, "Calculating interface

resistance”,

http://www.thermalengineer.com/library/calculating_interface_resistance.htm,

Last accessed November 6th, 2010.